



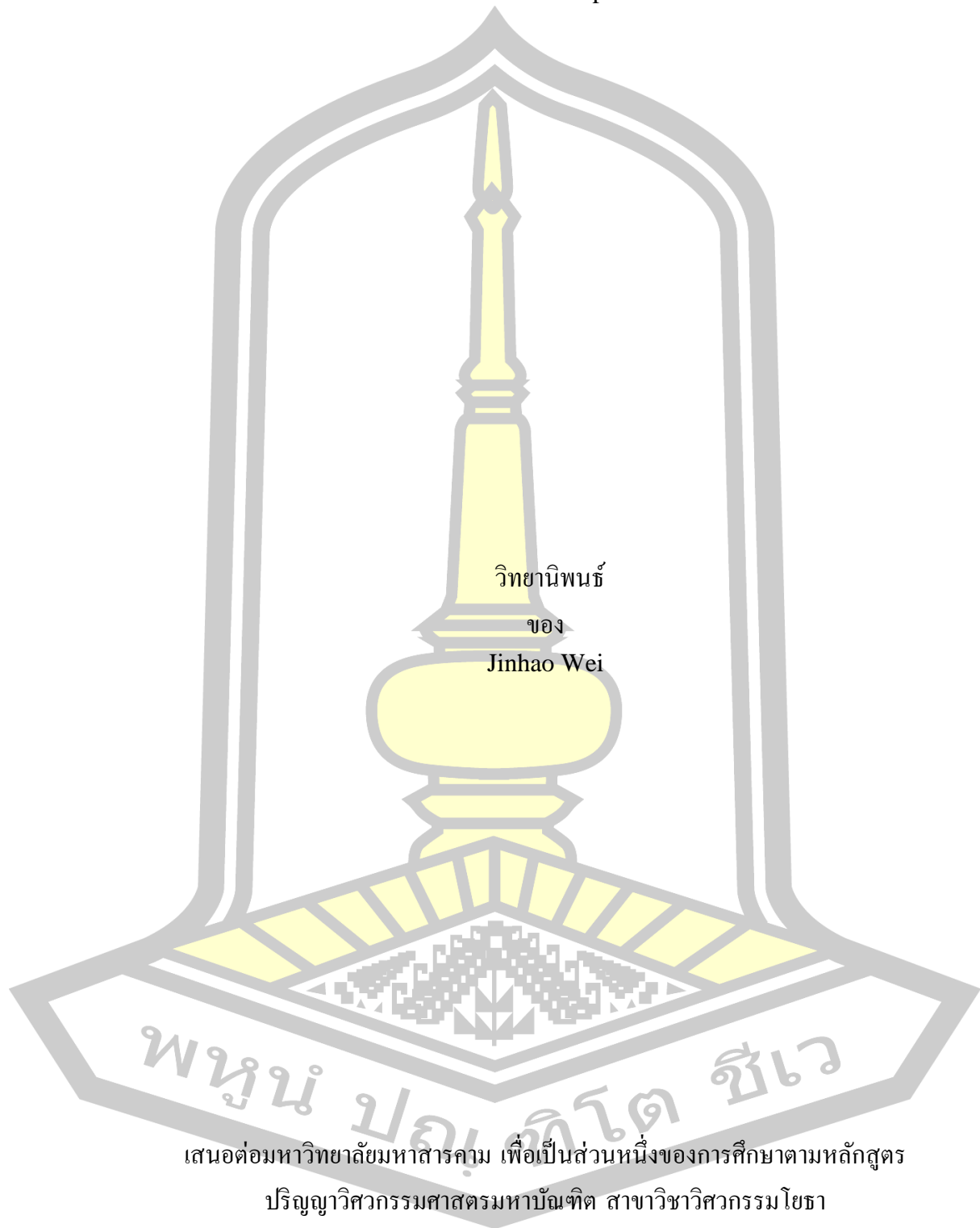
Reactive Powder Concrete Containing Fly Ash: Mixing Technique Effects and  
Mechanical Properties

Jinhao Wei

A Thesis Submitted in Partial Fulfillment of Requirements for  
degree of Master of Engineering in Civil Engineering  
November 2024

Copyright of Mahasarakham University

Reactive Powder Concrete Containing Fly Ash: Mixing Technique Effects and  
Mechanical Properties



วิทยานิพนธ์

ของ

Jinhao Wei

เสนอต่อมหาวิทยาลัยมหาสารคาม เพื่อเป็นส่วนหนึ่งของการศึกษาตามหลักสูตร

ปริญญาวิศวกรรมศาสตรมหาบัณฑิต สาขาวิชาวิศวกรรมโยธา

พฤษภาคม 2567

ลิขสิทธิ์เป็นของมหาวิทยาลัยมหาสารคาม

Reactive Powder Concrete Containing Fly Ash: Mixing Technique Effects and  
Mechanical Properties

Jinhao Wei

A Thesis Submitted in Partial Fulfillment of Requirements  
for Master of Engineering (Civil Engineering)

November 2024

Copyright of Mahasarakham University



The examining committee has unanimously approved this Thesis, submitted by Mr. Jinhao Wei , as a partial fulfillment of the requirements for the Master of Engineering Civil Engineering at Mahasarakham University

Examining Committee

Chairman

(Asst. Prof. Vatwong Greepala ,  
Ph.D.)

Advisor

(Assoc. Prof. Krit Chaimoon ,  
Ph.D.)

Committee

(Assoc. Prof. Raungrut Cheerarot ,  
Ph.D.)

Committee

(Assoc. Prof. Sahalaph  
Homwouttiwong , Ph.D.)

Mahasarakham University has granted approval to accept this Thesis as a partial fulfillment of the requirements for the Master of Engineering Civil Engineering

(Assoc. Prof. Juckamas Laohavanich ,  
Ph.D.)

(Assoc. Prof. Krit Chaimoon , Ph.D.)  
Dean of Graduate School

Dean of The Faculty of Engineering

พหุ ม ปรณ จิต ชีเว

<b>TITLE</b>	Reactive Powder Concrete Containing Fly Ash: Mixing Technique Effects and Mechanical Properties		
<b>AUTHOR</b>	Jinhao Wei		
<b>ADVISORS</b>	Associate Professor Krit Chaimoon , Ph.D.		
<b>DEGREE</b>	Master of Engineering	<b>MAJOR</b>	Civil Engineering
<b>UNIVERSITY</b>	Maharakham University	<b>YEAR</b>	2024

### ABSTRACT

This study explores the development of reactive powder concrete (RPC), which is known for its high mechanical properties and durability beyond conventional concrete. RPC has a unique composition including cement, silica fume, fine sand, superplasticizer, water and steel fibers. However, its performance is greatly affected by factors such as ingredient selection, mixing method and curing technology. Fly ash is a by-product of coal combustion and has the potential to serve as a partial cement replacement, enhancing the performance of RPC while reducing cost and environmental impact. However, the challenges of blending RPC, especially those with low water-to-cement ratios, remain significant and research on the mechanical properties of RPC containing fly ash is still limited.

This study aimed to (1) evaluate suitable mixing techniques for fly ash-containing RPC and (2) analyze their mechanical properties under selected mixing methods. Single-batch and double-batch techniques were studied, as well as the effects of single- and mixed-size steel fibers and different mixing temperatures. Double batching has been shown to significantly improve performance, mixed size fibers improve compressive strength, and single size fibers increase flow. However, high mixing temperatures reduce workability. The compressive strength, splitting tensile strength, and flexural strength of RPC containing fly ash were evaluated under double batches and compared with the ACI 318 standard and relevant literature.

**Keyword :** Reactive powder concrete (RPC), Fly ash, Mixing techniques, Double-batching, Splitting tensile strength, Flexural strength

## ACKNOWLEDGEMENTS

The author would like to sincerely thank Mahasarakham University for its support for this research and for giving the author the opportunity to study. This thesis was completed under the careful guidance of my advisor, Assoc. Prof. Krit Chaimoon. From the selection of the graduation thesis topic, to the research and demonstration of the topic, to the writing and revision of the thesis, every step has the careful guidance and serious analysis of the advisor. There were many difficulties encountered in the process of implementing the research, but they were gradually solved under the guidance of the advisor, which made me improve in all aspects. I would like to sincerely thank my advisor. At the same time, I would like to thank all the professional teachers who have educated me and provided help. The professional knowledge you imparted is the source of my continuous growth and the basis for completing this thesis. I would also like to thank my labmates for helping me solve problems when I encountered difficulties. In addition, I would like to thank all the scholars involved in this thesis. This thesis quotes the research literature of many scholars. Without the help and inspiration of the research results of various scholars, it would be difficult for me to complete the writing of this thesis. Finally, I would like to thank my family for their tolerance, care and encouragement during this period. It is because of their support and care that I can study with peace of mind and successfully complete my studies.

This graduation thesis not only improved my ability to think independently and solve problems, but also cultivated a serious, rigorous and meticulous learning attitude.

Graduation is imminent. In my future work and life, I will remember the teachings of my teachers and continue to work hard. I also wish all those who have helped me all the best.

Jinhao Wei

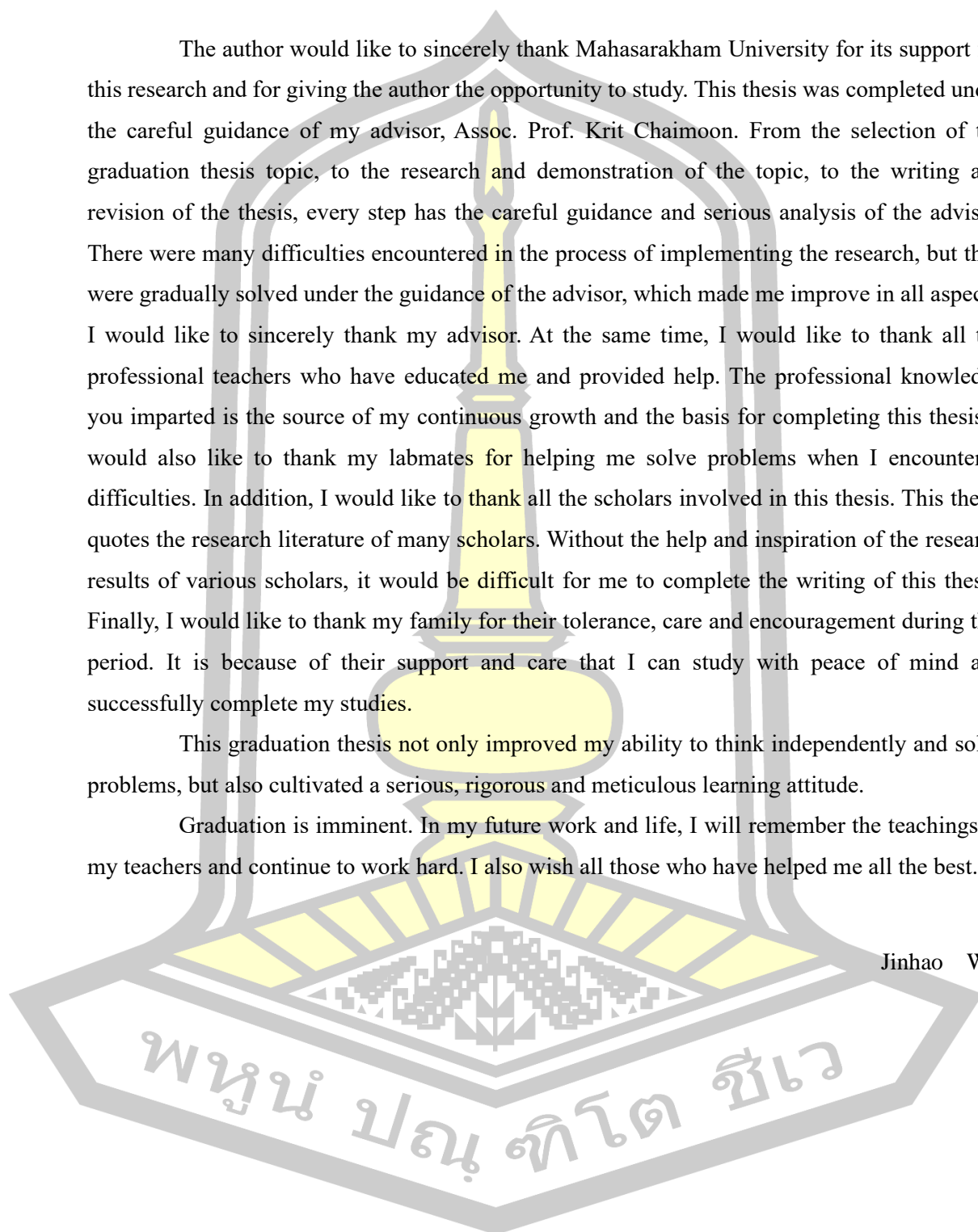


## TABLE OF CONTENTS

	<b>Page</b>
ABSTRACT.....	D
ACKNOWLEDGEMENTS.....	E
TABLE OF CONTENTS.....	F
LIST OF TABLES.....	K
LIST OF FIGURES .....	L
 Chapter 1	
Introduction.....	1
1.1 Problem Statement.....	1
1.2 Research Objectives .....	2
1.3 Research Scope.....	2
1.4 Expected Advantages .....	2
 Chapter 2	
Literature Review.....	3
2.1 Ultra-high Performance Concrete.....	3
2.1.1 Development of UHPC .....	3
2.1.2 Material Composition of UHPC.....	4
2.2 Reactive Powder Concrete.....	4
2.3 Steel Fiber.....	5
2.3.1 Types of Steel Fiber .....	5
2.3.1.1 Micro Steel Fiber .....	5
2.3.1.2 Macro Steel Fiber.....	5
2.3.1.3 Wavy Steel Fiber.....	6
2.3.1.4 Hooked-End Steel Fiber.....	6
2.3.1.5 Straight Steel Fiber .....	6
2.3.1.6 Stainless Steel Fiber.....	7
2.4 RPC with Steel Fiber and Other Fibers .....	7

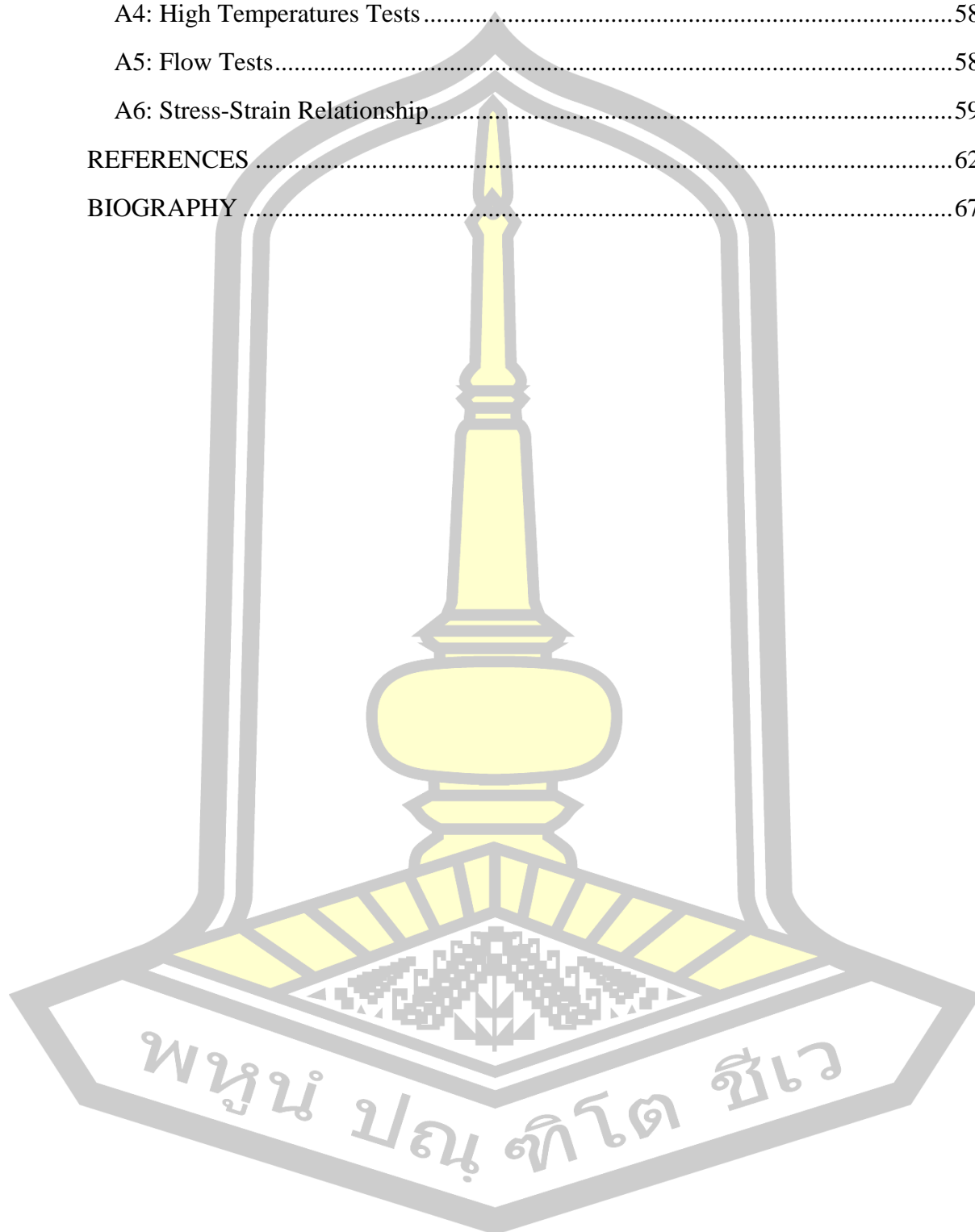
2.4.1 RPC with Steel Fiber .....	8
2.4.1.1 Compressive Strength of STF-RPC .....	8
2.4.1.2 Tensile Strength of STF-RPC .....	8
2.4.1.3 Flexural Strength of STF-RPC.....	9
2.4.2 RPC with Hybrid Polypropylene Fiber and Steel Fiber .....	9
2.4.2.1 Compressive Strength of PPF-STF-RPC .....	9
2.4.2.2 Tensile Strength of PPF-STF-RPC .....	9
2.4.2.3 Flexural Strength of PPF-STF-RPC.....	9
2.4.3 RPC with Hybrid Polyvinyl Alcohol Fiber and Steel Fiber .....	10
2.4.3.1 Compressive Strength of PVAF-STF-RPC .....	10
2.4.3.2 Tensile Strength of PVAF-STF-RPC .....	10
2.4.3.3 Flexural Strength of PVAF-STF-RPC .....	10
2.4.4 RPC with Hybrid Carbon Fiber and Steel Fiber.....	10
2.4.4.1 Compressive Strength of CF-STF-RPC.....	10
2.4.4.2 Tensile Strength of CF-STF-RPC .....	11
2.4.4.3 Flexural Strength of CF-STF-RPC .....	11
2.4.5 RPC with Hybrid Carbon Nano-Fiber and Steel Fiber.....	11
2.4.5.1 Compressive Strength of CNF-STF-RPC.....	11
2.4.5.2 Tensile Strength of CNF-STF-RPC .....	11
2.4.5.3 Flexural Strength of CNF-STF-RPC .....	12
2.5 Fly Ash.....	12
2.5.1 Sources and Formation of Fly Ash.....	12
2.5.2 Chemical Composition of Fly Ash.....	12
2.5.3 Physical Properties of Fly Ash .....	13
2.5.4 Reaction Mechanism of Fly Ash.....	14
2.5.5 Fly Ash for RPC Applications.....	15
2.5.5.1 Improvement of Long-term Compressive Strength of RPC ....	15
2.5.5.2 Improvement of Splitting Tensile Strength of RPC .....	15
2.5.5.3 Improvement of Flexural Strength of RPC.....	16



2.5.5.4 Retarding the Heat of Hydration of RPC .....	16
2.5.5.5 Improving the Resistance of RPC to Sulfate Attack .....	16
2.5.5.6 Improved Economic and Environmental Benefits .....	16
2.6 UHPC Mixing Method .....	17
2.6.1 Single-batch Mixing Method.....	17
2.6.2 Multi-batch Mixing Method.....	17
2.6.2.1 Advantages of the Multi-batch Mixing Method.....	18
2.6.2.2 Limitations of the Multi-batch Mixing Method.....	18
2.7 Relationships between Strengths of Concrete .....	18
2.7.1 Compressive Strength and Splitting Tensile Strength Relationship .....	18
2.7.2 Compressive Strength and Flexural Strength Relationship.....	19
Chapter 3	
Research Methods .....	20
Part I: Effects of Mixing Techniques.....	20
3.1 Raw Materials for Part I .....	20
3.2 Mix Proportion for Part I .....	23
3.3 Mixing Techniques Investigated.....	24
3.3.1 Single-Batching Method.....	24
3.3.2 Double-Batching Method .....	25
3.4 Specimen Preparation and Tests for Part I .....	26
Part II: Mechanical Properties of RPC Containing Fly Ash.....	27
3.5 Experimental Program for Part II .....	27
3.6 Mix Proportions for Part II .....	28
3.7 Specimen Preparation for Part II .....	28
3.8 Testing of Hardened RPC.....	30
3.8.1 Compressive Strength Test.....	30
3.8.2 Splitting Tensile Strength Test .....	31
3.8.3 Flexural Strength Test .....	32
Chapter 4	
Test Results and Analysis .....	34

4.1 Part I: Effects of Mixing Techniques.....	34
4.1.1 Effects of Mixing Methods.....	34
4.1.2 Effects of Type of Steel Fiber .....	36
4.1.3 Effects of Mixing Temperature on Flow Value of RPC .....	38
4.2 Part II: Mechanical Properties of RPC Containing Fly Ash.....	39
4.2.1 Density.....	39
4.2.2 Compressive Strength.....	39
4.2.3 Split Tensile Strength .....	41
4.2.4 Flexural Strength .....	43
4.2.5 Effects at High Temperatures.....	45
Chapter 5	
Conclusions.....	48
5.1 Part I: Effects of Mixing Techniques.....	48
5.1.1 Mixing Methods .....	48
5.1.2 Steel Fiber Types.....	48
5.1.3 Mixing Temperature and Flow Value .....	48
5.2 Part II: Mechanical Properties of RPC Containing Fly Ash.....	48
5.2.1 Density.....	48
5.2.2 Compressive Strength at 3 and 28 Days.....	48
5.2.3 Splitting Tensile Strength.....	48
5.2.4 Flexural Strength .....	49
5.2.5 Performance at High Temperatures.....	49
5.3 Suggestion.....	49
5.3.1 Optimization of Fly Ash Content and Environmental Benefits .....	49
5.3.2 Application Areas.....	49
5.3.3 Future Research.....	49
Appendix A: Pictures of the Tests .....	50
A1: Compression Strength Tests .....	50
A2: Splitting Tensile Strength Tests.....	54

A3: Flexural Strength Tests .....	56
A4: High Temperatures Tests .....	58
A5: Flow Tests.....	58
A6: Stress-Strain Relationship.....	59
REFERENCES .....	62
BIOGRAPHY .....	67



## LIST OF TABLES

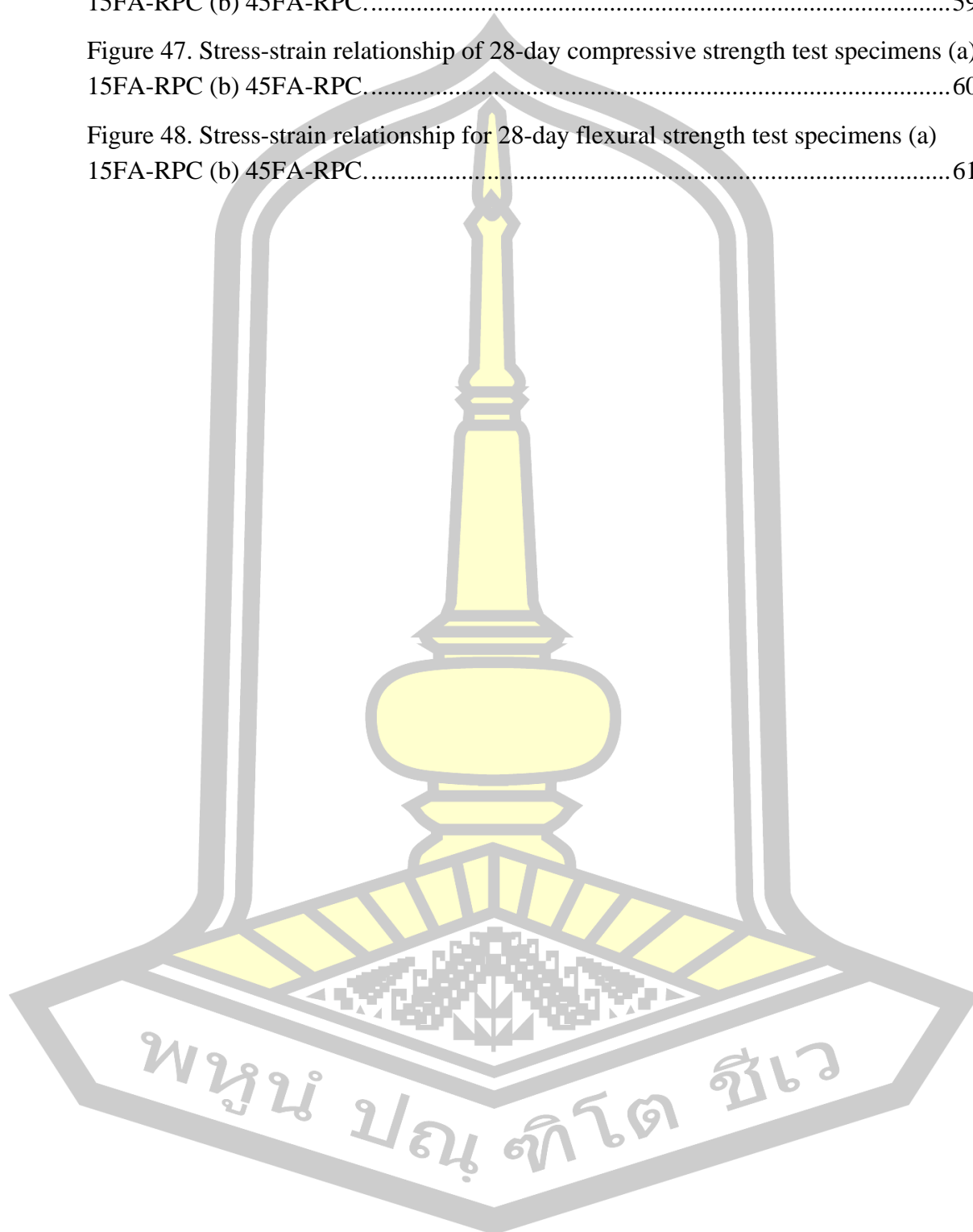
	Page
Table 1. RPC mechanical characteristics and typical composition [22] .....	4
Table 2. Performance of RPC with different fiber combinations .....	8
Table 3. Chemical composition of Class F fly ash [44] .....	13
Table 4. Chemical composition of Class C fly ash [45] . .....	13
Table 5. Physical properties of fly ash [44] . .....	14
Table 6. Compositions of RPC for Part I (kg/m <sup>3</sup> ). .....	23
Table 7. Experimental program for Part II.....	28
Table 8. Compositions of RPC for Part II (kg/m <sup>3</sup> ). .....	28
Table 9. Results of RPC mixing at a constant temperature of 25°C.....	35
Table 10. Flow values of RPC with different mixing temperatures. ....	38
Table 11. Density for RPC with different fly ash contents.....	39
Table 12. Compressive strength of RPC with 15%FA and 45%FA using double-batching method.....	40
Table 13. Splitting tensile strength of RPC with 15%FA and 45%FA using double-batching method.....	41
Table 14. The relationship between the ratio of splitting tensile strength to compressive strength in this study and related literature. ....	43
Table 15. Flexural strength of RPC with 15%FA and 45%FA using double-batching method.....	43
Table 16. The relationship between the ratio of flexural strength to compressive strength in this study and related literature. ....	45

## LIST OF FIGURES

	Page
Figure 1. The development of concrete compressive strength for over 100 year [21] .	3
Figure 2. Wavy steel fiber [26] .....	6
Figure 3. Hooked-end steel fiber [26] .....	6
Figure 4. Straight steel fiber.....	7
Figure 5. Straight steel fiber [27].....	7
Figure 6. Distribution and particle shape of fly ash [43] .....	12
Figure 7. Mechanism of the activation of fly ash particles [46] .....	14
Figure 8. Mechanism of the hydration of PC+FA [46] .....	15
Figure 9. Raw materials. ....	21
Figure 10. Comparison of single and mixed size fiber. ....	21
Figure 11. SEM images of cement, fly ash, and silica fume. ....	23
Figure 12. Single- and double- batching methods (modified from [15]).....	24
Figure 13. Mixing all binders and sand in a tray. ....	25
Figure 14. Adding steel fiber and continue mixing. ....	25
Figure 15. The 5 litre standard mixer from MD Supply Ltd. ....	26
Figure 16. Flow testing. ....	26
Figure 17. Specimen preparation for Part I.....	27
Figure 18. The 20 litre standard mixer from Bosson Ltd in Thailand. ....	29
Figure 19. Example of Specimen preparing for Part II.....	29
Figure 20 . Specimen curing (Part II). ....	30
Figure 21. Compression test according to: (a) ASTM C109 and (b) ASTM C39.....	31
Figure 22. Splitting tensile strength test according to ASTM C496.....	32
Figure 23. Two-point Flexural Strength testing.....	33
Figure 24. Flexural strength test according to ASTM C1609.....	33
Figure 25. Effect of mixing method on RPC compressive strength. ....	35

Figure 26. Samples with single-batching method for compression test: (a) before testing and (b) after testing .....	36
Figure 27. Samples with double-batching method for compression test: (a) before testing and (b) after testing .....	36
Figure 28. Effects of type of steel fiber on RPC compressive strength. ....	37
Figure 29. Samples with mixed-size fibers for compression test: (a) before testing and (b) after testing .....	37
Figure 30. Samples with single-size fibers for compression test: (a) before testing and (b) after testing .....	38
Figure 31. Comparison of 3-day and 28-day compressive strength. ....	40
Figure 32. 28 days splitting tensile strength. ....	42
Figure 33. 28 days flexural strength. ....	44
Figure 34. Temperature-time curves for different target temperatures using oven heating.....	46
Figure 35. Explosive spalling of samples at high temperatures.....	46
Figure 36. D-M-15FA-30GS70NS samples for 3 days compressive strength testing:(a) before testing and (b) after testing .....	51
Figure 37. D-M-45FA-30GS70NS samples for 3 days compressive strength testing:(a) before testing and (b) after testing .....	51
Figure 38. D-M-15FA-30GS70NS samples for 28 days compressive strength testing:(a) before testing and (b) after testing .....	52
Figure 39. D-M-45FA-30GS70NS samples for 28 days compressive strength testing:(a) before testing and (b) after testing .....	53
Figure 40. D-M-15FA-30GS70NS samples for 28 days splitting tensile strength testing:(a) before testing and (b) after testing .....	54
Figure 41. D-M-45FA-30GS70NS samples for 28 days splitting tensile strength testing:(a) before testing and (b) after testing .....	55
Figure 42. D-M-15FA-30GS70NS samples for 28 days flexural strength testing:(a) before testing and (b) after testing .....	56
Figure 43. D-M-45FA-30GS70NS samples for 28 days flexural strength testing:(a) before testing and (b) after testing .....	57
Figure 44. Post-explosion samples. ....	58
Figure 45. Flow test results.....	59

Figure 46. Stress-strain relationship of 3-day compressive strength test specimens (a) 15FA-RPC (b) 45FA-RPC.....	59
Figure 47. Stress-strain relationship of 28-day compressive strength test specimens (a) 15FA-RPC (b) 45FA-RPC.....	60
Figure 48. Stress-strain relationship for 28-day flexural strength test specimens (a) 15FA-RPC (b) 45FA-RPC.....	61





# Chapter 1

## Introduction

### 1.1 Problem Statement

Reactive powder concrete (RPC) is an ultra-high performance fiber reinforced concrete (UHPFRC) having superior structural properties [1]. RPC originally consists of cement, silica fume, fine sand, steel fiber, superplasticizer, and water [2]. Excluding of coarse aggregate and use of a high amount of binder allows RPC to attain ultra-high strength. However, the high strength of RPC makes it extremely brittle. Therefore, commonly fiber are added into the mixture (ranging from 1.5 to 3% in vol.) in an attempt of decreasing its brittleness [2].

Given that fiber constitute one of the fundamental materials employed by RPC and are typically expensive. A substantial body of research has been conducted in academic institutions on the enhancement of fiber. Among the areas of research, the enhancement of the mechanical properties and strain-hardening behaviour of RPC by steel fiber has been the subject of extensive investigation [3, 4].

The addition of steel fiber has a significant improvement for concrete in terms of strength, toughness and plasticity. Some experimental studies have shown that with the increase in the volume ratio of steel fiber, steel fiber reinforced concrete performance increases more significantly. However, the steel fiber is not the more you use the better [5, 6]. On the one hand, steel fiber is expensive, mixing too much will increase the project cost. On the other hand, the slender steel fiber is flexible, easy to form clusters, the volume rate is too high, it will not be able to give full play to its reinforcing effect. In order to improve the reinforcing effect of steel fiber and meet its construction performance, steel fiber is usually used with a length of 10 mm to 60 mm, a diameter or equivalent diameter from 0.2 mm to 1 mm, a length-to-diameter ratio of 30 to 100, and a volume rate of 0.5% to 2%. The length-to-diameter ratio is 30 to 100, and the volume ratio is 0.5 to 2 percent. Additionally, the geometry and type of steel fiber have a considerable influence on the performance of concrete. It has been observed that the length, configuration and content of steel fiber in concrete have a considerable impact on the load-carrying capacity, toughness and post-peak behaviour of concrete [7-10]. Furthermore, some researchers have investigated the impact of combining distinct fiber types into hybrid fiber on concrete. This approach aims to leverage the unique roles of each fiber type in concrete and to optimise the benefits of steel fiber in concrete. For instance, Kang et al [11] and Lawler et al [12] demonstrated that the incorporation of hybrid fiber effectively enhanced the tensile properties of concrete.

Nevertheless, despite the superior mechanical properties of activated powder concrete in comparison to ordinary concrete, its cost is also considerably higher, which has thus far limited its development. This has prompted numerous scholars to investigate the development of more cost-effective and environmentally friendly materials with the objective of reducing their production costs. As a by-product of thermal power plants, fly ash can be employed as a partial substitute for cement in concrete, thereby reducing the quantity of other materials, such as cement, and



consequently the overall material cost [13]. Furthermore, the incorporation of a specific proportion of fly ash has been demonstrated to enhance the flexural and splitting tensile strength of RPC [14]. This improvement may be attributed to the filling effect of the fine particles, which reduces the porosity and increases the density and strength of the material.

Another major challenge in the application of RPC in structures is the large-scale production [15]. As the production volumes of RPC increase, the mixing of the batch using standard mixers becomes challenging due to the fact that the required mixing torque exceeds the capacity of the standard mixers [16]. The cost of a high-energy mixer is approximately 20 times that of a standard mixer using a high-strength mixer with a higher torque capacity [17]. To address this challenge, Du et al [15] investigated the mixing dynamics of UHPC. Their findings demonstrated that the multi-batch mixing approach effectively reduced the peak mixing torque of UHPC without significantly compromising its critical performance.

Although the use of fly ash can reduce the production cost of RPC and the multi-batch mixing method is suitable for high-volume production, current research lacks a systematic exploration of the use of this combination of the two. Further research into the benefits and optimisation of this combination is necessary to improve the economics and operability of RPC and to promote their wider application in real-world production.

## **1.2 Research Objectives**

The principal objective of this study is to examine the mechanical properties of RPC containing fly ash, with two specific sub-objectives as outlined below.

1) To select a suitable mixing technique by investigating effects of mixing techniques on properties of RPC containing fly ash. The main parameters include mixing methods, fiber types, and mixing temperatures.

2) Using the appropriate mixing technique obtained, to investigate mechanical properties of RPC containing different amounts of fly ash. The mechanical properties evaluated include 3-day and 28-day compressive strengths, 28-day splitting tensile strength, and 28-day flexural strength. The 28-day compressive strengths at high temperatures are also determined.

## **1.3 Research Scope**

1) Based on previous studied [18, 19], the replacement of cement with fly ash was performed at 15% and 45% of the total weight of both materials.

2) To ensure suitability for use as repair concrete, the flow value was controlled to be in a range of  $200 \pm 10$  mm to  $250 \pm 10$  mm by adjusting superplasticizer dosage.

## **1.4 Expected Advantages**

1) A better understand on mechanical properties of RPC containing fly ash.

2) A better understand on the effects of mixing techniques on properties of RPC containing fly ash.

## Chapter 2

### Literature Review

#### 2.1 Ultra-high Performance Concrete

Ultra-high performance concrete (UHPC) is a high-strength, highly durable cementitious material with significant advantages over other types of concrete such as high compressive strength, high tensile strength, and ductility under tensile loads. Currently, UHPC is used in many countries including China, the United States, Australia, Germany, Italy, France and Japan. The application of UHPC is becoming more and more popular, and engineers in various countries are constantly improving the performance and economy of this new material [20].

##### 2.1.1 Development of UHPC

The importance of concrete in the construction industry has been increasingly emphasized as a major material that has been added to the construction field in recent times, and in the 1930s intensive attempts were made by scientists to improve the compressive strength of concrete. Figure 1 shows the development of the compressive strength of concrete during the 20th century. It is clear from the graph that concrete technology progressed slowly in the 1960s.

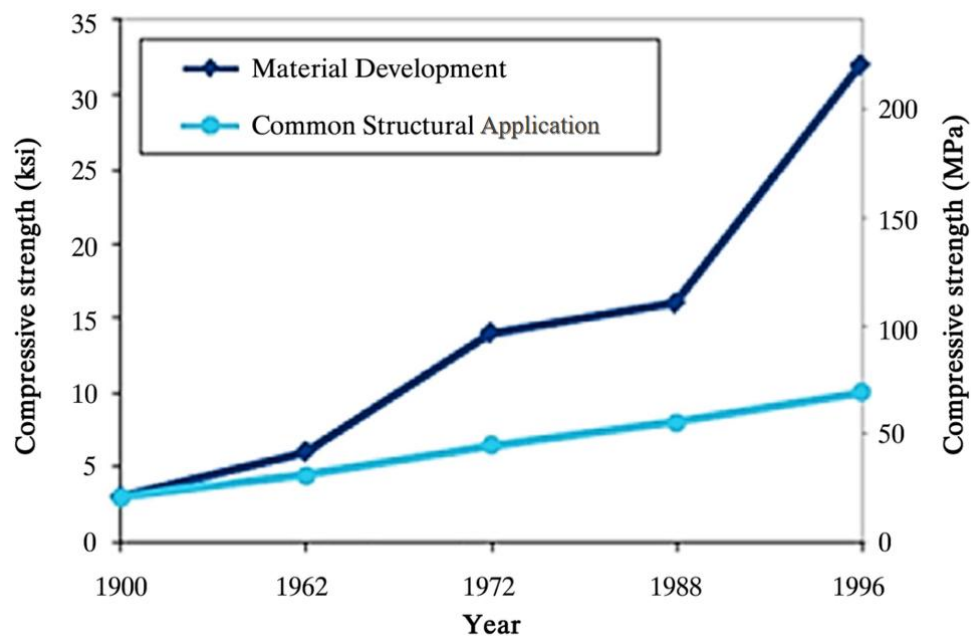


Figure 1. The development of concrete compressive strength for over 100 year [21] .

The main reason for this was due to the technical barriers of water reducing agents until the superplasticizer (SP) was discovered and proved to be effective in

reducing the values of water to binder ratio (w/b). Since then the compressive strength of concrete has been significantly improved.

### 2.1.2 Material Composition of UHPC

The constituents of UHPC include cementitious components, quartz powder, quartz sand, superplasticizer, admixtures, water, and fiber. Quartz sand constitutes the largest granular elements in the UHPC skeleton, while quartz powder is used as a filler due to its fine dimensions.

## 2.2 Reactive Powder Concrete

Reactive powder concrete (RPC) was a significant development in the creation of UHPC during the 1990s. It was first developed in the early 1990s at the Bouygues Laboratory in France. Its concept is based on arranging multiple particles in a dense manner. RPC is the most commonly used type of UHPC in laboratory and field tests due to its high binder content, very low water-to-cement ratio, and the use of silica fume (SF), fine quartz powder, quartz sand and superplasticizer. According to the composition and method of thermal processing, the compressive strength of RPC ranges from 200 MPa to 800 MPa. Table 1 presents the typical composition and mechanical properties of RPC [22]. RPC has better usability than its predecessors. This ease of characterization is an advantage and a crucial criterion for large-scale cementitious material applications.

Table 1. RPC mechanical characteristics and typical composition [22] .

Material	Characteristics	RPC200	RPC800
Cement	Portland cement—type V (ASTM C150)	955	1000
Sand	Fine sand (150–400 m)	1050	5000
Silica fume	Silica fume (18 m <sup>2</sup> /g)	229	390
Precipitated silica	Precipitated silica (35 m <sup>2</sup> /g)	10	230
Super plasticizer	Super plasticizer (polyacrylate)	13	18
Steel fiber	Steel fibers (length 3 mm and diameter 180 um)	191	630
Water	Total water	153	180
Typical Mechanical Properties of Reactive Powder Concrete (MPa)			
Compressive strength	Compressive strength (cylinder)	170–230	490–680
Flexural strength	Flexural strength	25–30	45–102
Young's modulus		54–60	

## 2.3 Steel Fiber

Since the advent of RPC in the early 1990s, it has been found that RPC tend to exhibit very brittle properties, and it has also been found that the mechanical properties of RPC can be improved by adding various fiber materials to them. In practical applications around the world, steel fiber (STF) are one of the most commonly used fiber added to RPC, and are also the most commonly used type of material in fiber reinforced materials. STF are usually short and thin, made of high-strength steel with a diameter of 0.20-0.75 mm. STF has a high density. The density of STF is typically in the range of 7.8 to 7.9 g/cm, which is higher than that of other fiber materials, such as glass fiber and carbon fiber. This high density results in better dispersion and homogeneity of STF in concrete, which improves the strength and durability of concrete. Secondly, STF has excellent tensile strength. After special treatment, STF can significantly increase the tensile strength of concrete and improve its crack resistance. Compared with conventional concrete, adding STF at the same volume ratio can increase the tensile strength of concrete by more than 30%. This makes STF a very effective reinforcing material that can improve the overall mechanical properties of concrete structures. As a result, the addition of STF to concrete can inhibit microcracking due to applied loads or shrinkage [23-25] and exhibit excellent performance after high temperatures [6, 24], and is therefore widely used in bridges, tunnels, large buildings and other projects requiring high strength and durability, also can improve the safety and service life of infrastructure projects. However, the efficacy of this material is contingent upon a number of factors, including the quantity and type of STF, the mixing methods employed, the maintenance conditions, the mix design, and other variables.

### 2.3.1 Types of Steel Fiber

The introduction of steel fiber in both UHPC and RPC has greatly improved the mechanical properties and durability of the material. The commonly seen types of steel fiber include micro steel fiber, macro steel fiber, corrugated steel fiber, end hook steel fiber, linear steel fiber, high strength steel fiber, and stainless steel fiber.

#### 2.3.1.1 Micro Steel Fiber

Micro steel fiber is typically 0.2-0.5 mm in diameter and 6-13 mm in length. These fibers, due to their fine size, can be uniformly distributed in the RPC matrix, significantly improving the crack resistance and toughness of the material. Micro steel fiber is mainly used in engineering applications where high surface quality and uniform properties are required.

#### 2.3.1.2 Macro Steel Fiber

Macro steel fiber typically have a diameter of 0.5-1 mm and a length between 25-60 mm. Due to their large size, macro steel fiber can significantly enhance the impact resistance of RPC and reduce crack propagation in mass concrete structures. These fibers are commonly used in bridges and high-rise buildings in critical structural areas.

### 2.3.1.3 Wavy Steel Fiber

Wave steel fiber have a unique wave shape that gives them a stronger bond and grip in the concrete matrix. This shape makes corrugated steel fiber particularly good at improving the tensile strength and overall toughness of RPC for applications where high crack resistance is required. Wave steel fiber is shown in Figure 2.

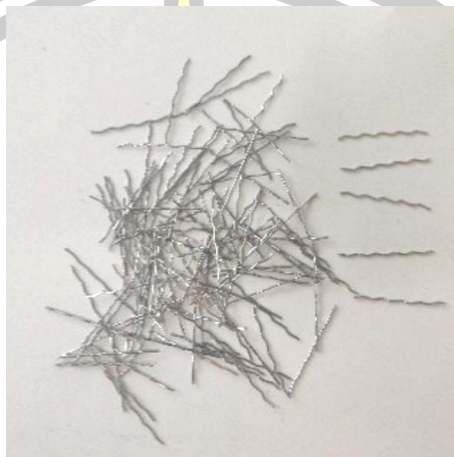


Figure 2. Wavy steel fiber [26] .

### 2.3.1.4 Hooked-End Steel Fiber

The two ends of the end hook steel fiber have a hook-shaped design, which enhances the anchoring ability of the fiber in concrete. This kind of fiber performs well in improving the bending strength and crack resistance of RPC, and is widely used in key structures such as bridge decks and tunnel linings. Hooked-end steel fiber is shown in Figure 3.



Figure 3. Hooked-end steel fiber [26] .

### 2.3.1.5 Straight Steel Fiber

Straight steel fiber is one of the simplest types and does not have any special shape design. Although it does not bond to the concrete matrix as well as corrugated or end-hooked steel fiber, straight steel fiber can still provide some reinforcement in



certain less demanding applications, especially in cost-sensitive projects. Straight steel fiber is shown in Figure 4.



Figure 4. Straight steel fiber.

#### 2.3.1.6 Stainless Steel Fiber

Stainless steel fiber is manufactured from stainless steel materials for excellent corrosion resistance. In marine structures or chemical plants, stainless steel fiber protects RPC from corrosive substances and extend service life, making them the material of choice for extreme environments. Stainless steel fiber is shown in Figure 5.



Figure 5. Straight steel fiber [27].

### 2.4 RPC with Steel Fiber and Other Fibers

The Steel Fiber Reinforced Reactive Powder Concrete (STF-RPC) is a high performance concrete. The addition of STF to concrete improves its mechanical properties, such as tensile strength, toughness, and ductility, while combining it with other materials or adding other fiber enhances other properties of the concrete. For example, corrosion resistance, electrical conductivity, etc. Table 2 compares the main characteristics of STF-RPC with those of other RPC with different fiber.

Table 2. Performance of RPC with different fiber combinations

Property	STF-RPC	PPF-STF-RPC	PVAf-STF-RPC	CF-STF-RPC	CNF-STF-RPC
Compressive Strength (MPa)	100-200 <sup>[28]</sup>	151.2 <sup>[29]</sup>	84.5-128.6 <sup>[30]</sup>	162-165 <sup>[31]</sup>	170 <sup>[32]</sup>
Tensile Strength (MPa)	5-15 <sup>[33]</sup>	17.9 <sup>[29]</sup>	24.3 <sup>[29]</sup>	4.5-8.5 <sup>[30]</sup>	7.5-9.5 <sup>[34]</sup>
Flexural Strength (MPa)	20-50 <sup>[35]</sup>	32.4 <sup>[29]</sup>	11.7-20.07 <sup>[36]</sup>	25 <sup>[31]</sup>	21.7 <sup>[32]</sup>

#### 2.4.1 RPC with Steel Fiber

The effect of STF on the compressive strength of RPC depends on the volume fraction and type of STF used. A study found that increasing the volume fraction of STF from 1 to 4% increased the compressive strength [37]. In a separate study, RPC was examined with varying volume fractions of STF, including 0%, 2%, 3%, and 4% [35]. The results indicated that compressive strength increased as the dosage of STF increased. Ju et al. [38] found that a volume fraction of 1.5% resulted in better compressive strength than smaller fractions of STF. Similarly, Tai et al. [28] and Abid et al. [39] reported normal temperature and residual compressive strength (after exposure to elevated temperatures) of RPC with a volume fraction of 2% STF.

##### 2.4.1.1 Compressive Strength of STF-RPC

The compressive strength of STF-RPC is influenced by a number of factors including the type and amount of STF, mix design and curing conditions. In general, the addition of STF can significantly increase the compressive strength of RPC.

Studies have shown that the compressive strength of STF-RPC can range from 100 MPa to 200 MPa or more, depending on factors such as STF content. The data are presented in Table 2. For example, one study found that STF-RPC with a STF content of 2% had higher compressive strengths at ambient and elevated temperatures than RPC with 1% STF and 3% STF [28].

Overall, STF-RPC is a promising material for high performance and durable concrete structures, and its compressive strength can be significantly improved by the addition of STF and appropriate curing conditions.

##### 2.4.1.2 Tensile Strength of STF-RPC

As common, the tensile strength of STF-RPC is usually lower than its compressive strength, but the addition of STF can significantly increase its tensile strength.

Typically, the tensile strength of STF-RPC can range from 5 MPa to 15 MPa or more, depending on the STF content and other factors. See Table 2 for data. For example, one study showed that the tensile strength of STF-RPC with 0.5%, 1% and 1.5% by volume of STF increased with increasing STF content [33]. Curing conditions and the type of STF used also affect the tensile strength of STF-RPC.

#### **2.4.1.3 Flexural Strength of STF-RPC**

The flexural strength of STF-RPC is also influenced by a number of factors including STF content, aspect (L/D) and curing conditions.

In general, the flexural strength of STF-RPC can range from 20 MPa to 50 MPa or more, depending on the STF content and other factors [35].

The aspect ratio of the STF also affects the flexural strength of STF-RPC. In general, STF with a higher aspect ratio increase the flexural strength of STF-RPC. However, too high an aspect ratio can lead to fiber balling and agglomeration, which can reduce the effectiveness of the reinforcement.

Curing conditions also affect the flexural strength of STF-RPC. High pressure curing is considered to be an effective method of improving the flexural strength of STF-RPC as it improves the bond between the STF and the cementitious matrix.

#### **2.4.2 RPC with Hybrid Polypropylene Fiber and Steel Fiber**

Polypropylene fiber (PPF) is a synthetic fiber made from polypropylene polymer. It is characterised by low weight, high strength, corrosion and abrasion resistance and good durability. The addition of PPF to concrete can improve the crack resistance and impact strength of concrete. It has been found that the addition of appropriate amounts of PPF, STF and fiber blend combinations (PPF + STF) can prevent explosive spalling [40].

##### **2.4.2.1 Compressive Strength of PPF-STF-RPC**

The compressive strength of PPF-RPC is significantly lower than that of STF-RPC and PPF-STF-RPC due to the lower strength and modulus of PPF compared to STF [41].

Studies have shown that the compressive strength of PPF-STF-RPC can be 151.2 MPa or more [29]. See Table 2 for data.

##### **2.4.2.2 Tensile Strength of PPF-STF-RPC**

Due to the additional tensile strength provided by PPF, previous studies have shown that RPC with only one of the added PPF performs poorly compared to PPF-STF-RPC [29]. Due to the superior microstructure of PPF-STF-RPC and the combined effect of the fiber, its tensile and splitting tensile strengths at ambient temperature were higher than those of RPC with only one of the fiber added.

Studies have shown that the tensile strength of PPF-STF-RPC can be 17.9 MPa or more [29]. The data is shown in Table 2.

##### **2.4.2.3 Flexural Strength of PPF-STF-RPC**

Adding PPF and STF to RPC increases its flexural strength compared to regular RPC without fiber. The addition of PPF and STF provides additional resistance to crack propagation. PPF play an important role in crack resistance, as they resist crack propagation, thus enhancing the flexural strength of RPC. The addition of steel fiber further enhances the flexural strength of RPC compared to PPF alone.

Studies have shown that the flexural strength of PPF-STF-RPC can be 32.4 MPa or more [29]. The data is shown in Table 2.



### **2.4.3 RPC with Hybrid Polyvinyl Alcohol Fiber and Steel Fiber**

In concrete, PVAf is commonly used as reinforcing materials to improve the crack resistance and durability of concrete. PVAf also has a high modulus of elasticity, which helps to improve the crack control and ductility of concrete structures and improves the mechanical properties of concrete.

#### **2.4.3.1 Compressive Strength of PVAf-STF-RPC**

A study by Sanchayan et al. [41] investigated the compressive strength of six different RPC blends containing different percentages by volume of PVAf and STF. The results showed that replacing STF with PVAf does not affect the modulus of elasticity, but does adversely affect the strength of the RPC. However, replacing 50% of the STF with PVAf results in reasonable strengths.

Studies have shown that the compressive strength of PVAf-STF-RPC can range from 84.5 MPa to 128.6 MPa or more [30]. The data is shown in Table 2.

#### **2.4.3.2 Tensile Strength of PVAf-STF-RPC**

It has been shown that PVAf can increase the tensile strength and toughness of concrete, and mixing PVAf with STF can effectively control the cracking and brittleness of concrete and increase the strength of concrete [29]. Among them, the mixing with the best test results could reach a tensile strength of 24.3 MPa. The data is shown in Table 2.

#### **2.4.3.3 Flexural Strength of PVAf-STF-RPC**

Flexural strength of PVAf-STF reinforced polymer concrete is also discussed in related studies [42]. Addition of PVAf and STF to the concrete mixture increased the flexural strength of the concrete. It was also found that the flexural strength of PVAf-STF-RPC increased with increase in fiber volume fraction.

Studies have shown that the flexural strength of PVAf-STF-RPC can range from 11.7 MPa to 20.07 MPa or more [36]. The data is shown in Table 2.

### **2.4.4 RPC with Hybrid Carbon Fiber and Steel Fiber**

RPC with hybrid carbon fiber and steel fiber (CF-STF-RPC) is a hybrid fiber reinforced high performance concrete. CF and STF have high strength and toughness respectively, and their combination can significantly improve the tensile strength and toughness of RPC, thus improving its overall performance. In addition, CF has excellent electrical conductivity, which can improve the electrical conductivity of RPC, and it also has good high temperature stability, which allows RPC to maintain its performance in high temperature environments. The use of CF as a reinforcing material for RPC offers the potential for lightweight, durable and high performance concrete.

#### **2.4.4.1 Compressive Strength of CF-STF-RPC**

It is known that the compressive strength of RPC is increased by the addition of STF. Similarly, the addition of CF to RPC increases the compressive strength due to the high tensile strength and high modulus of the CF.

The compressive strength of CF-STF-RPC varies depending on the ratio of carbon to STF and the concrete matrix in which the CF are embedded. It is important to note that the compressive strength of CF-STF-RPC can be carefully blended and optimised to meet the requirements of a specific application.

Studies have shown that the compressive strength of CF-STF-RPC can range from 162 MPa to 165 MPa or more [31]. The data is shown in Table 2.

#### **2.4.4.2 Tensile Strength of CF-STF-RPC**

CF-STF RPC exhibited higher tensile strength than normal RPC, especially at high temperatures. The hybridisation of 0.5% CF and 1.5% STF had a synergistic effect on tensile strength. The addition of hybrid fiber also contributed significantly more to tensile strength than to compressive strength. A study by Wang et al. [30] reported that the addition of CF and STF to RPC resulted in a significant increase in the tensile strength of the material. It was found that the tensile strength of RPC increased from 4.5 MPa to 8.5 MPa with the addition of 1% CF and 1% STF. The data is shown in Table 2.

#### **2.4.4.3 Flexural Strength of CF-STF-RPC**

The combination of CF and STF in RPC has a positive effect on the flexural strength of concrete compared to plain RPC. The experimental study by Raza et al. [31] showed that the flexural strength of blended CF-STF-RPC at normal and high temperatures is significantly higher than that of plain RPC, and the blended fiber mixture of 1.5STF-0.5CF-RPC has the highest flexural strength of 25MPa. The data is shown in Table 2.

#### **2.4.5 RPC with Hybrid Carbon Nano-Fiber and Steel Fiber**

RPC with hybrid carbon nano-fiber and steel fiber (CNF-STF-RPC) is a high performance concrete reinforced with a blend of nanoscale carbon fiber and steel fiber. Due to the nanoscale size and porous structure of CNF, CNF have a high specific surface area and can be used as catalyst carriers, adsorbent materials and electrode materials.

In the field of concrete, CNF are commonly used as reinforcing materials. The use of CNF in RPC can potentially improve its durability and crack resistance, as CNF have been shown to enhance the interfacial bonding between the fiber and the matrix, thus improving stress transfer and crack resistance. Therefore, CNF has a broad application prospect in the field of construction materials.

##### **2.4.5.1 Compressive Strength of CNF-STF-RPC**

It has been shown that the introduction of CNF into UHPC doped with STF increases the compressive strength up to a maximum value of 170 MPa [32]. However, CNF is more advantageous in terms of economic benefits compared to carbon nanotubes, and the introduction of CNF promotes the interaction of STF with the cement matrix, thus reducing the required dose of STF.

##### **2.4.5.2 Tensile Strength of CNF-STF-RPC**

The tensile strength of CNF-STF-RPC varies according to the ratio of CNF to STF. A study by Yu et al. [34] found that the addition of CNF and STF to UHPC resulted in a significant increase in the tensile strength of the material. It was found that the optimum fiber content for UHPC was 2% of the fiber volume, when the tensile strength was 7.5-9.5 MPa. The data is shown in Table 2.

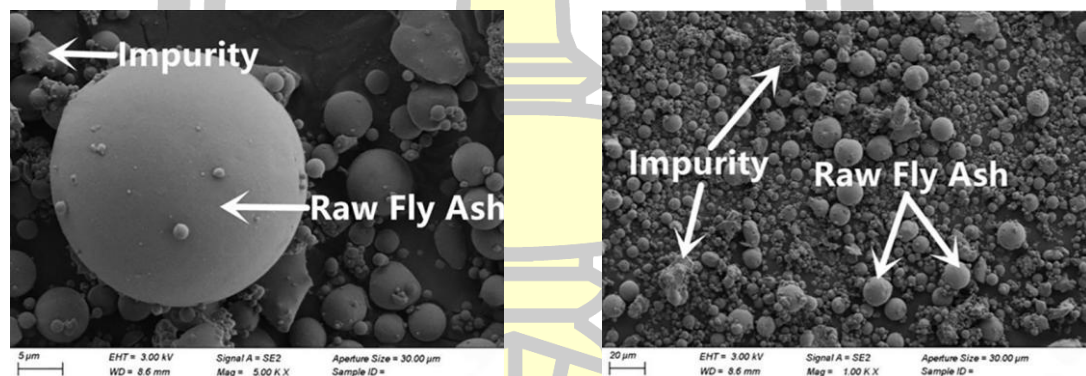
### 2.4.5.3 Flexural Strength of CNF-STF-RPC

Adding CNF and STF to UHPC can significantly increase the flexural strength. Research by Sbia et al. [32] shows that using the best combination of STF and CNF can make the maximum flexural strength of ordinary UHPC reach 21.7MPa. This is mainly due to the reinforcing effects of CNF and STF at different scales, where CNF mainly slows down the formation and propagation of microcracks, while STF mainly hinders the growth and opening of larger cracks.

## 2.5 Fly Ash

### 2.5.1 Sources and Formation of Fly Ash

Fly ash (FA) is a fine particulate matter collected from flue gas after coal combustion and represents an important industrial byproduct. The primary source of FA is the flue gas purification process employed in coal-fired thermal power plants. When coal is burned at elevated temperatures, the inorganic materials present, including silicon, aluminum, iron, and calcium, undergo a phase transition to form small particles in a molten state. These particles rapidly cool and solidify within the flue gas stream, resulting in the formation of FA. The particles typically exhibit a spherical morphology and range in size from 1 to 100 microns. The microscopic enlargement is shown in Figure 6.



(a) Spherical particle morphology (b) particle size distribution of fly ash  
Figure 6. Distribution and particle shape of fly ash [43] .

### 2.5.2 Chemical Composition of Fly Ash

The main components of FA include silicates, aluminates, iron oxides, calcium oxides, magnesium oxides, etc., which give fly ash-based cements their properties. The specific composition depends on the type of coal combustion and combustion conditions, usually FA has a higher content of silica and aluminum trioxide. Depending on the calcium content, FA can be divided into two categories:

Class F is produced primarily through the combustion of low-calcium coals, including anthracite and bituminous coal. These coals possess a high silica and aluminum trioxide content, rendering them suitable for use in concrete that is resistant to sulfate attack. Its main chemical components are shown in Table 3.

Table 3. Chemical composition of Class F fly ash [44] .

SiO <sub>2</sub> %	69.35%
Al <sub>2</sub> O <sub>3</sub> %	16.37%
Fe <sub>2</sub> O <sub>3</sub> %	3.72%
CaO%	3.02%
MgO%	0.57%
SO <sub>3</sub> %	0.29%
Na <sub>2</sub> O%	1.50%
K <sub>2</sub> O%	1.05%
MnO%	0.045%
LOI%	4.27%

Class C is primarily produced by the combustion of high-calcium coals, such as lignite, which contain a high concentration of calcium oxide and exhibit self-hardening properties. This class of concrete is suitable for applications requiring high strength. Its main chemical components are shown in Table 4.

Table 4. Chemical composition of Class C fly ash [45] .

SiO <sub>2</sub>	46.59%
Al <sub>2</sub> O <sub>3</sub>	12.42%
Fe <sub>2</sub> O <sub>3</sub>	9.74%
CaO	14.50%
MgO	7.23%
SO <sub>3</sub>	5.52%
Na <sub>2</sub> O	1.01%
K <sub>2</sub> O	2.28%

### 2.5.3 Physical Properties of Fly Ash

The shape and particle size of FA particles have a significant impact on its application in concrete. The spherical morphology of the majority of FA particles contributes to the fluidity and workability of concrete. Furthermore, the finer nature of FA particles, coupled with their higher specific surface area, enables them to fill smaller pores and enhance the compactness of concrete, as compared to cement. The common physical properties of FA are detailed in Table 5.

Table 5. Physical properties of fly ash [44] .

Physical appearance	Powder's
The color	Gray
Capacity mass (g/cm <sup>3</sup> )	2.1
Specific surface (cm <sup>2</sup> /g)	2950
Flexural (MPa)	2.9±0.4
Compressive (MPa)	6.5±0.2

#### 2.5.4 Reaction Mechanism of Fly Ash

The primary reaction mechanism of FA in concrete is the volcanic ash reaction. The reaction of silica and alumina trioxide in FA with calcium hydroxide, produced by the hydration of cement in an alkaline environment, results in the breakdown of the Si-Al chain within the FA particles. This generates a significant number of reactive groups involved in the volcanic ash reaction, leading to the formation of a new hydration product, calcium silicate hydrate. This reaction enhances the strength and durability of concrete, both in terms of its ultimate strength and its resistance to chemical attack [46]. The reaction mechanism of fly ash in concrete is illustrated in Figure 7.

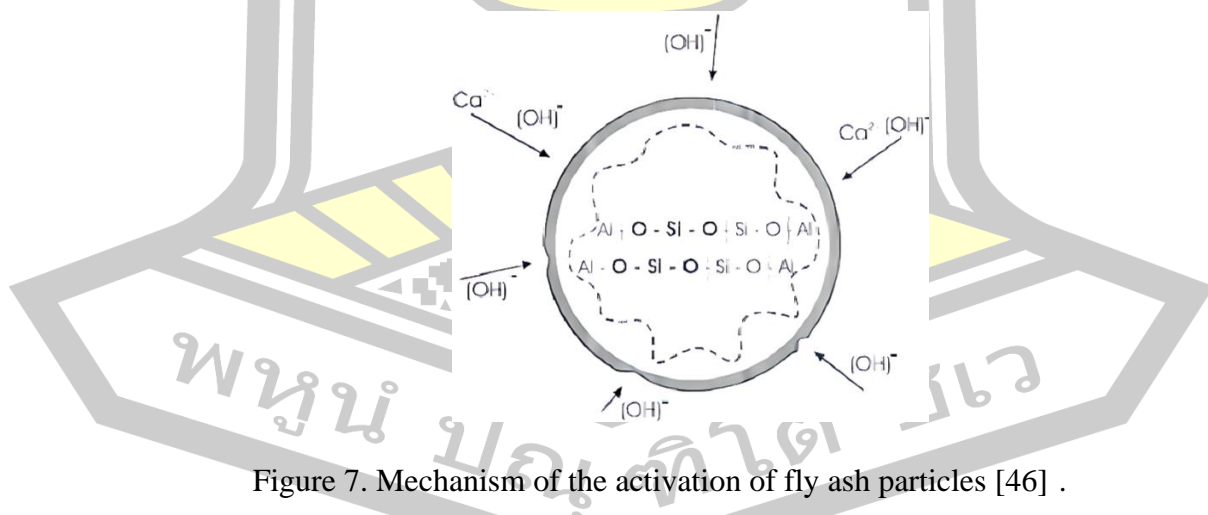


Figure 7. Mechanism of the activation of fly ash particles [46] .

The structure of the cement paste setting can be connected with the number of links between the cement particles. The hydration mechanism of Portland cement (PC) and fly ash mixture is shown in Figure 8.

As has already been stated, in the nucleation period, C-S-H, C-Al-H and Ca(OH)<sub>2</sub> are grouped around the fly ash particles, which act as crystallization centers.



As for the activated material, due to the increase of the free surface energy, an increased number of links between the activated Portland cement (APC) particles. The activated particles of fly ash (AFA), through the formed active groups, facilitate the establishment of a high number of links with the Portland cement particles.

Such a structure results in an increase of the mechanical characteristics of the mixture.

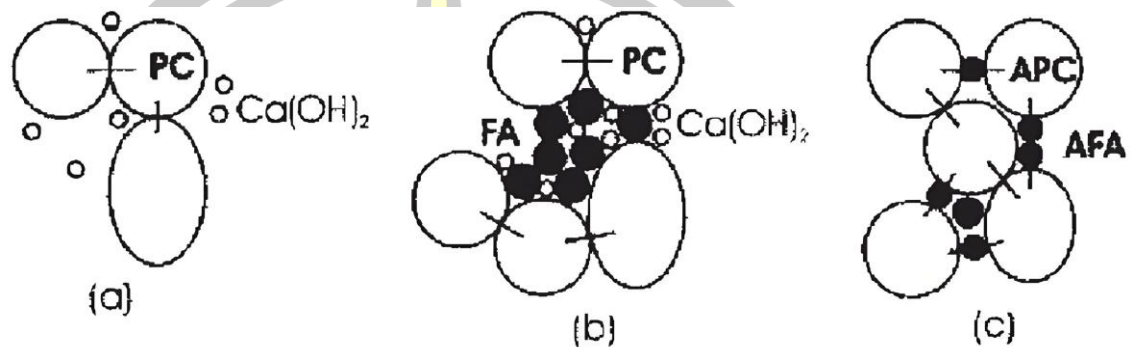


Figure 8. Mechanism of the hydration of PC+FA [46] .

### 2.5.5 Fly Ash for RPC Applications

The use of FA has multiple benefits, which can not only reduce costs, but also improve concrete performance and optimize construction operability with proper addition [47]. Therefore, the application of FA in building materials has received more and more attention.

#### 2.5.5.1 Improvement of Long-term Compressive Strength of RPC

There are differences in the effect of FA application in concrete on early and long-term compressive strength. Due to the reaction properties of volcanic ash, the hydration of FA in concrete is slower, resulting in a slower gain in strength of FA concrete, usually in the first 28 days. Several studies have shown that the compressive strength of FA concrete usually decreases in the early stages compared to that of all-cement concrete [46].

Although fly ash contributes less to the early strength, the volcanic ash activity in FA is gradually stimulated over time and reacts with calcium hydroxide  $\text{Ca(OH)}_2$  produced by cement hydration to produce additional C-S-H gel, which contributes to the densification and strength of the concrete. As a result, after prolonged curing, concrete containing FA can exhibit higher compressive strength, even exceeding that of ordinary concrete without FA. The specific effect depends on the amount of fly ash added, the concrete mixing ratio and the curing conditions [44, 48]. Therefore, in practice, the use of FA must be weighed against the early and long-term strength changes according to the project requirements.

#### 2.5.5.2 Improvement of Splitting Tensile Strength of RPC

The incorporation of FA not only enhances the compressive strength of concrete, but also the splitting tensile strength. Studies have shown that the moderate incorporation of FA can increase the densification of concrete, thereby reducing the generation of microcracks. Specifically, FA generates more C-S-H gels through volcanic ash reaction, and these gels fill the pores in the concrete, making the internal

structure of the material more dense, and the tensile strength is significantly improved. According to the relevant research, the splitting tensile strength of RPC can be increased by 48% with 8% of FA dosage at 28 days [49].

#### **2.5.5.3 Improvement of Flexural Strength of RPC**

FA also has a significant contribution in improving the flexural strength of RPC. Flexural strength is an important indicator of the resistance of concrete to bending stress, and the addition of FA enhances the flexural properties of concrete by improving the microstructure and compactness. Experimental data show that the addition of 30% FA can increase the flexural strength of RPC by about 10% [48], which is important for structural components subjected to high bending stresses.

#### **2.5.5.4 Retarding the Heat of Hydration of RPC**

FA can effectively retard the release of heat of hydration of concrete and reduce the occurrence of temperature cracks. Temperature cracking is a common problem in large volume RPC pours, especially at high heat of hydration. The low heat of hydration properties of FA can reduce the temperature rise rate of concrete during early hydration [13, 50], thereby reducing the internal and external temperature difference and the risk of crack formation. This gives FA a significant advantage in the application of large volume RPC structures.

#### **2.5.5.5 Improving the Resistance of RPC to Sulfate Attack**

The incorporation of FA represents an efficacious method for augmenting the chemical resistance of RPC, which is comprised of a considerable number of cementitious components and is therefore susceptible to sulfate attack. The volcanic ash reaction of FA diminishes the  $\text{Ca(OH)}_2$  content of the concrete, thereby reducing the potential for sulfate attack [51]. The addition of FA reduces the formation of internal sulfate crystals, thereby enhancing the durability of RPC. Concurrently, the fine particles in FA fill the pores in the concrete, which reduces its permeability and improves its corrosion resistance. Moreover, specific components in FA can react with foreign corrosive substances to form stable compounds, thus preventing further penetration of corrosive substances. This phenomenon is particularly evident in concrete structures used in harsh environments, such as marine environments.

#### **2.5.5.6 Improved Economic and Environmental Benefits**

The use of FA is a cost-effective alternative to traditional cement-based materials, with the partial replacement of cement in concrete formulations demonstrating the potential for significant cost savings. Concurrently, the utilisation of FA not only curtails the accumulation of solid waste and environmental pollution but also reduces the quantity of cement employed, consequently diminishing  $\text{CO}_2$  emissions. With the growing consciousness of environmental protection, the deployment of FA is progressively becoming the favoured green building material. The utilization of FA results in a reduction of approximately one ton of cement demand for each ton of FA employed, consequently leading to a reduction of approximately one ton of  $\text{CO}_2$  emissions [44]. This substitution not only contributes to the more efficient utilisation of solid waste, but also significantly reduces greenhouse gas emissions. The utilisation of FA in large-scale RPC applications serves to enhance the sustainability of construction works. This has resulted in a growing interest in the utilisation of FA in construction materials.

## 2.6 UHPC Mixing Method

The mixing methods for UHPC are different from those for conventional concrete, mainly mixing methods that properly mix ultra-fine powders and micro-aggregates to achieve its high strength and durability, including single-batch mixing and multi-batch mixing [15].

### 2.6.1 Single-batch Mixing Method

The traditional RPC mixing method mainly uses the single batch mixing method. Single batch mixing means that all the binders are added to the mixer at one time for mixing. The main steps are as follows.

1) Dry mixing: first pour the binders and sand into the mixer and dry mix, so that all kinds of dry materials are fully mixed.

2) Adding high efficient water reducing agent and water: add high efficient water reducing agent and mixing water slowly into the mixer, mixing to make the mixture gradually wet, to ensure that the water reducing agent and the dry materials are in full contact. Keep mixing until the mixture is homogenised.

3) Add steel fiber: Slowly and evenly add the steel fiber into the mixer. Continuous mixing ensures that the steel fiber are evenly distributed in the mix.

### 2.6.2 Multi-batch Mixing Method

Mixing UHPC with low w/c ratios results in different microstructure development and mixing torque requirements compared to conventional concrete. A major challenge in the structural application of UHPC is its large-volume production [52].

To address this issue, Du et al. investigated the mixing kinetics of UHPC, using a binder composed of Type I Portland cement, silica fume, and ground granulated blast furnace slag. They evaluated the effects of mixing temperature (10°C, 20°C, 30°C), mixing volume (1.5L, 3.0L, 4.5L, 6.0L), and mixing method (single-batching, double-batching, and triple-batching) on the mixing torque. Traditional RPC mixing uses a single-batching method, where all ingredients are combined in a single step. Their results showed that the multi-batch method significantly reduced the peak mixing torque of UHPC. The double-batch method reduced it by 44%, and the three-batch method reduced it by 59%. However, its key performance has not been significantly reduced. Therefore, the multi-batch method is expected to achieve large-scale production of UHPC.

Multi-batch mixing means that the ingredients are added to the mixer in batches and mixed several times. The main steps are as follows.

1) Material pre-mixing: according to the concrete proportion design, prepare the required raw materials, and then dry mix the binders and sand.

2) The first batch of materials added: Firstly, half of the mixed bonding agent and sand with mixing water and high-efficiency water reducing agent are added to the mixer. Start mixing to ensure that these materials are initially mixed well.

3) The second batch of materials to join: when the first batch of materials to achieve a certain degree of mixing, add the remaining half of the bonding agent and sand with mixing water and high-efficiency water reducing agent. Continue mixing so that all materials are well mixed.



4) Final mixing and discharging: add steel fiber into the mixer. Once all the materials have been added and mixed well, continue mixing for a while to ensure overall uniformity and then pour out the mixed concrete.

#### **2.6.2.1 Advantages of the Multi-batch Mixing Method**

In general, higher fluidity can be achieved by mixing UHPC using the multi-batch method. Higher fluidity means that the concrete is easier to construct and vibrate, can better fill formwork and small voids, and improves the overall workability and construction performance of the concrete. Multi-batch mixing also avoids the problem of localized uneven mixing that occurs in a single large-scale mixing operation, thereby improving the uniformity of the concrete. In addition, multi-batch mixing can effectively reduce the peak torque demand of the mixer, extend the service life of the equipment, and reduce energy consumption.

#### **2.6.2.2 Limitations of the Multi-batch Mixing Method**

Although the double batch mixing method helps improve fluidity, if the mixing time, speed and material delivery of each batch are not completely consistent, it may still lead to uneven material properties, affecting the final quality and consistency. In addition, the double batch mixing method has higher technical requirements for construction personnel, requiring operators to have richer experience and higher skill levels. This may require additional training and management, increasing the complexity and cost of construction management. The management and use of materials also require more sophisticated control to avoid material waste and incorrect delivery. Any material waste or misoperation will directly affect the construction cost and final quality.

### **2.7 Relationships between Strengths of Concrete**

#### **2.7.1 Compressive Strength and Splitting Tensile Strength Relationship**

The relationship between compressive strength and splitting tensile strength in concrete is well-established in both research and design standards. According to ACI 318-08, the splitting tensile strength  $f_t$  can be approximately calculated as:

$$f_t \approx 0.56f_c'^{0.5} \quad (2.1)$$

where  $f_c'$  is the compressive strength of concrete (in MPa). This formula is based on empirical studies and is generally applied for normal-weight concrete [53]. The equation illustrates that tensile strength is proportional to the square root of compressive strength, which aligns with the fact that tensile strength in concrete is much lower than compressive strength due to the brittle nature of the material.

Empirical studies further show that this relationship holds across a range of normal-strength concrete mixes, though it may vary for high-strength concrete. The value of 0.56 is an average coefficient that can shift depending on mix design, aggregate type, and curing conditions. While splitting tensile strength testing can be challenging, this equation provides a practical means for estimating tensile capacity based on compressive strength, aiding in simplified structural design. It was further shown in an evaluation and study of the ratio of split tensile strength to compressive

strength of concrete with cylindrical compressive strength up to 120 MPa by Nihal et al [54]. The relationship between splitting tensile strength and compressive strength can be expressed by the following formula:

$$f_t \approx (0.387f_c'^{-0.37})f_c' \quad (2.2)$$

### 2.7.2 Compressive Strength and Flexural Strength Relationship

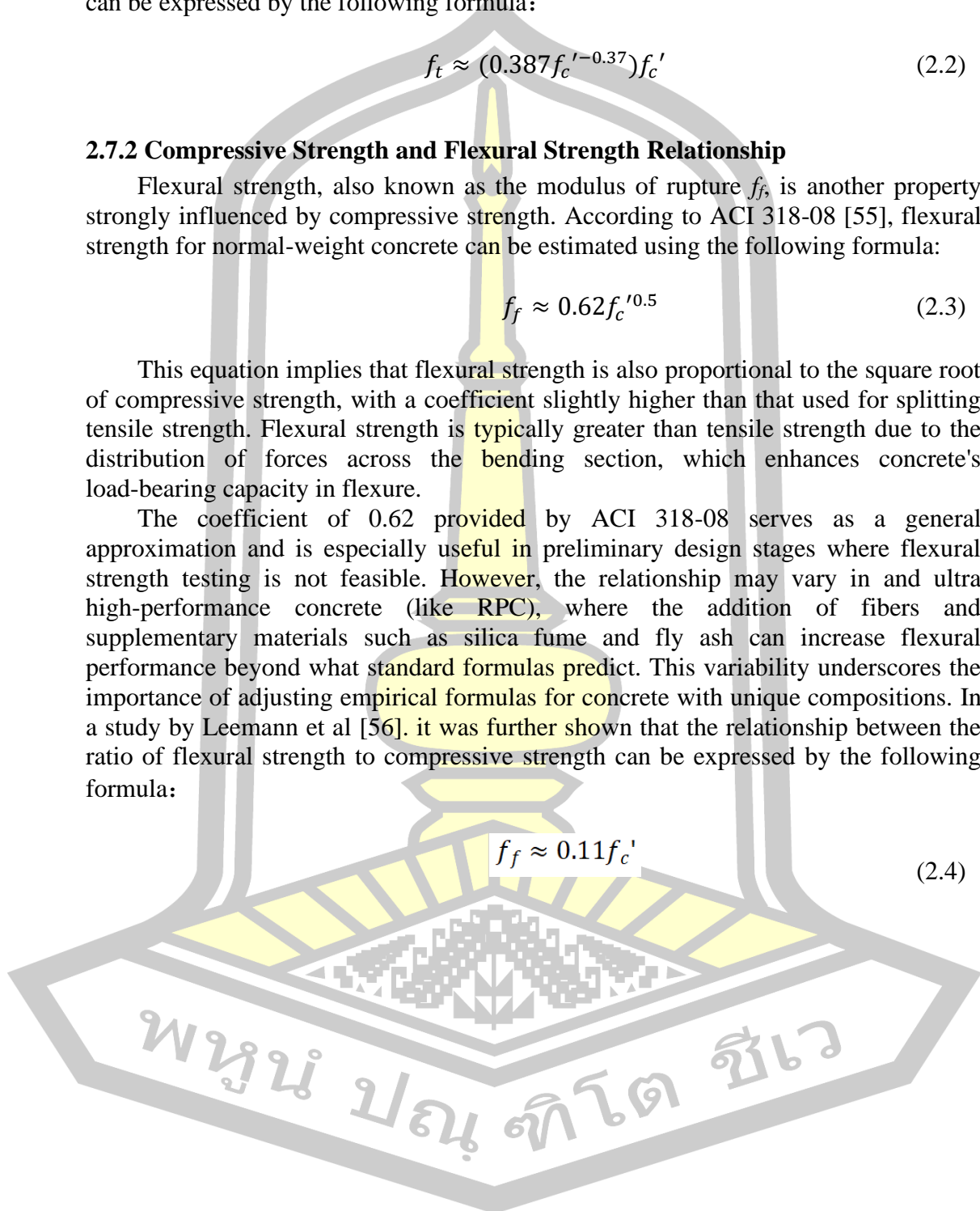
Flexural strength, also known as the modulus of rupture  $f_f$ , is another property strongly influenced by compressive strength. According to ACI 318-08 [55], flexural strength for normal-weight concrete can be estimated using the following formula:

$$f_f \approx 0.62f_c'^{0.5} \quad (2.3)$$

This equation implies that flexural strength is also proportional to the square root of compressive strength, with a coefficient slightly higher than that used for splitting tensile strength. Flexural strength is typically greater than tensile strength due to the distribution of forces across the bending section, which enhances concrete's load-bearing capacity in flexure.

The coefficient of 0.62 provided by ACI 318-08 serves as a general approximation and is especially useful in preliminary design stages where flexural strength testing is not feasible. However, the relationship may vary in and ultra high-performance concrete (like RPC), where the addition of fibers and supplementary materials such as silica fume and fly ash can increase flexural performance beyond what standard formulas predict. This variability underscores the importance of adjusting empirical formulas for concrete with unique compositions. In a study by Leemann et al [56], it was further shown that the relationship between the ratio of flexural strength to compressive strength can be expressed by the following formula:

$$f_f \approx 0.11f_c' \quad (2.4)$$



## Chapter 3

### Research Methods

In this study, there are two main parts including (1) studying the effects of mixing techniques on the properties of reactive powder concrete (RPC) containing fly ash to consider a suitable mixing technique and (2) investigating the mechanical properties of RPC containing fly ash using the appropriate mixing technique.

#### Part I: Effects of Mixing Techniques

##### 3.1 Raw Materials for Part I

The materials used in this part are as follows and as shown in Figure 9.

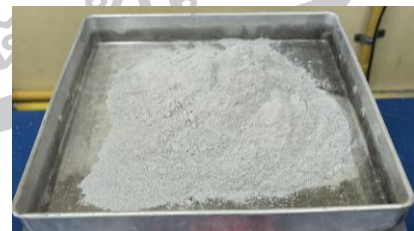
- 1) Cement (C) is hydraulic cement manufactured by Siam Cement Group, Thailand that meets TIS 2594-2556 industrial standards.
- 2) Silica fume (SF) is undensified silica fume provided by Eikem company, Thailand.
- 3) Fly ash (FA) is one provided by Taurus Pozzolan Company, Thailand that meets American Standard ASTM C 618-15.
- 4) Superplasticizer (SP) is polycarboxylate type.
- 5) Sand (S), in saturated surface dry condition, is graded river sand (GS) from Chi river, Thailand with sizes of 0.15 to 0.60 mm.
- 6) Water (W) is tap water.
- 7) Steel fiber (STF) is straight fiber, copper-plated fiber from China. Two types were considered.
  - a) Single-size fiber has a diameter of 0.22 mm and a length of 13 mm. Its aspect ratio or length-to-diameter ratio is 59.
  - b) Mixed-size fibers have diameters in a range from 0.18 mm to 0.35 mm and lengths between 12 mm and 14 mm. The aspect ratios vary from 37 to 78, with an average of 56.

Detailed comparison differences are shown in Figure 10.

The SEM images of C, SF, and FA are illustrated in Figure 11. It can be seen that C particles have an irregular shape, while both SF and FA particles have a rounded shape. SF particles have the smallest size.



(a) Hydraulic cement



(b) Silica fume



(c) Fly ash



(d) Superplasticizer



(e) Graded sand



(f) Tap water



(g) Single-size steel fiber

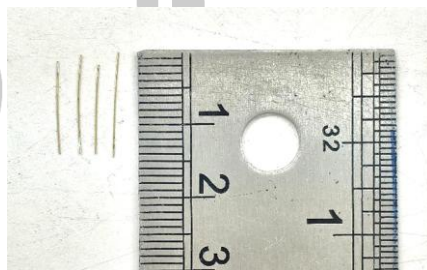


(h) Mixed-size steel fiber

Figure 9. Raw materials.



(a) Single-size steel fiber

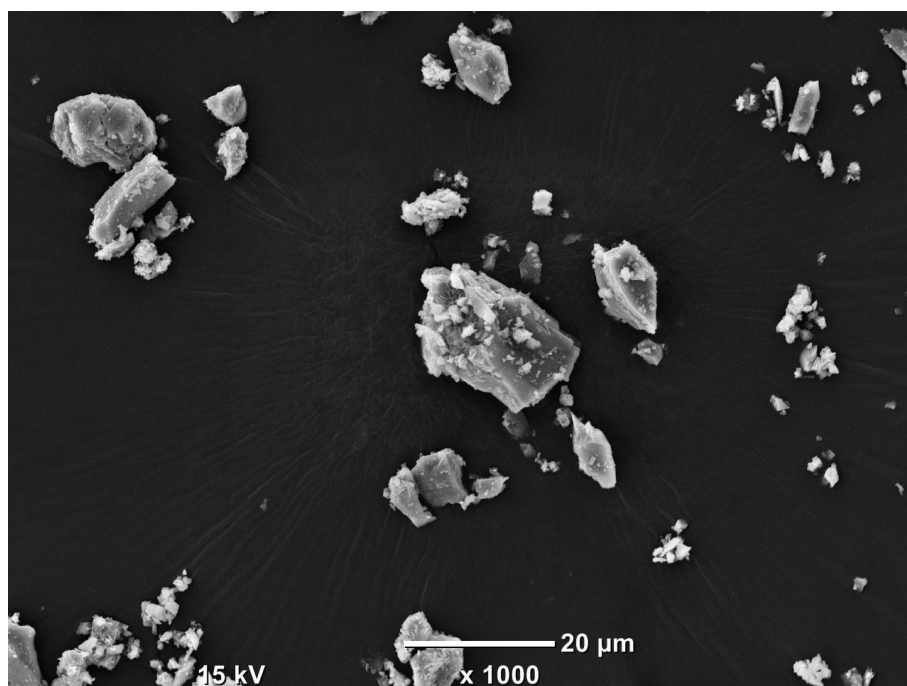


(b) Mixed-size steel fiber

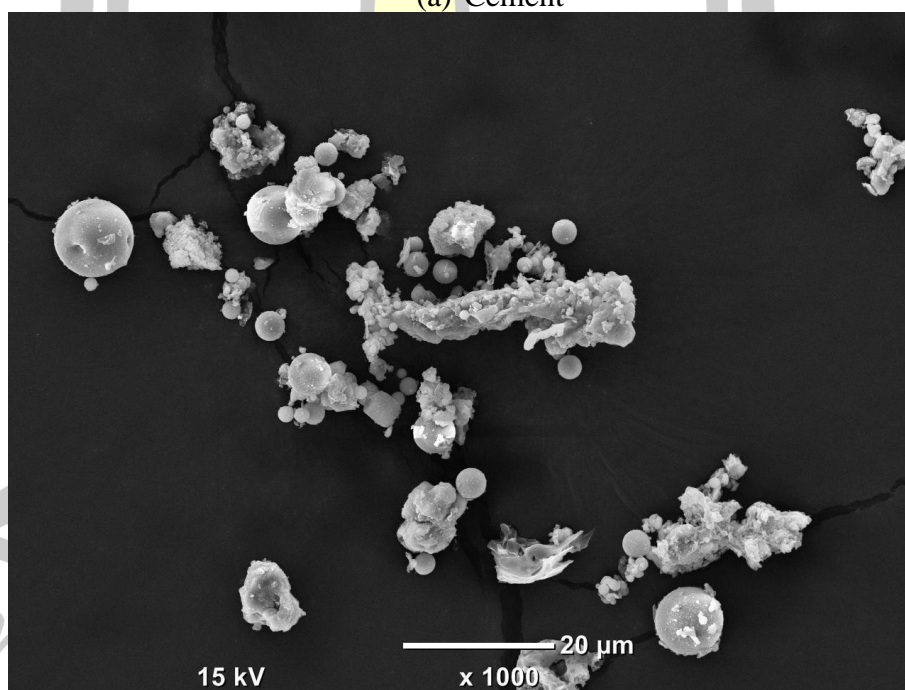
Figure 10. Comparison of single and mixed size fiber.



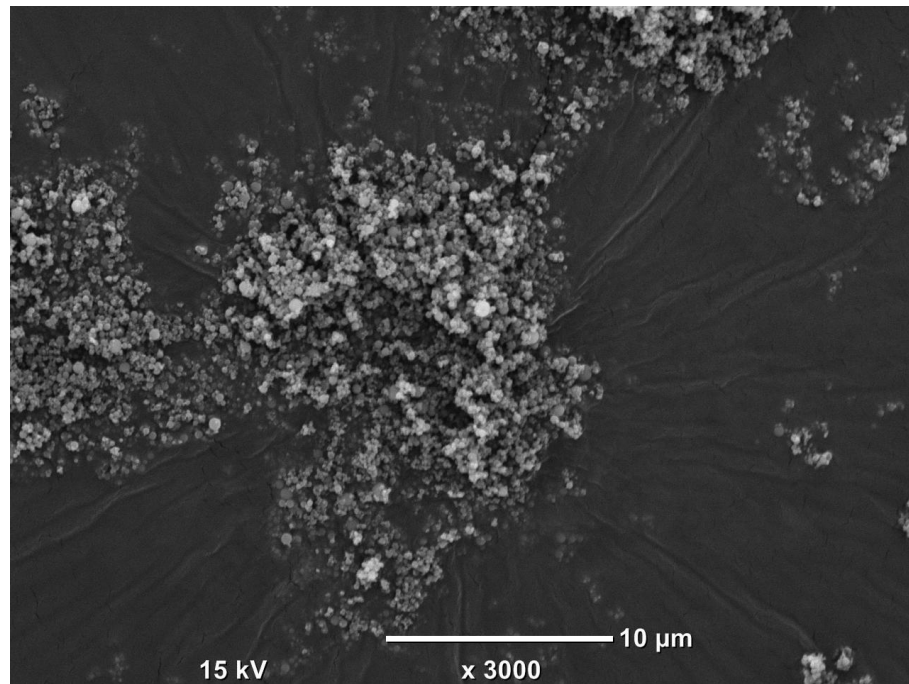




(a) Cement



(b) Fly ash



(c) Silica fume

Figure 11. SEM images of cement, fly ash, and silica fume.

### 3.2 Mix Proportion for Part I

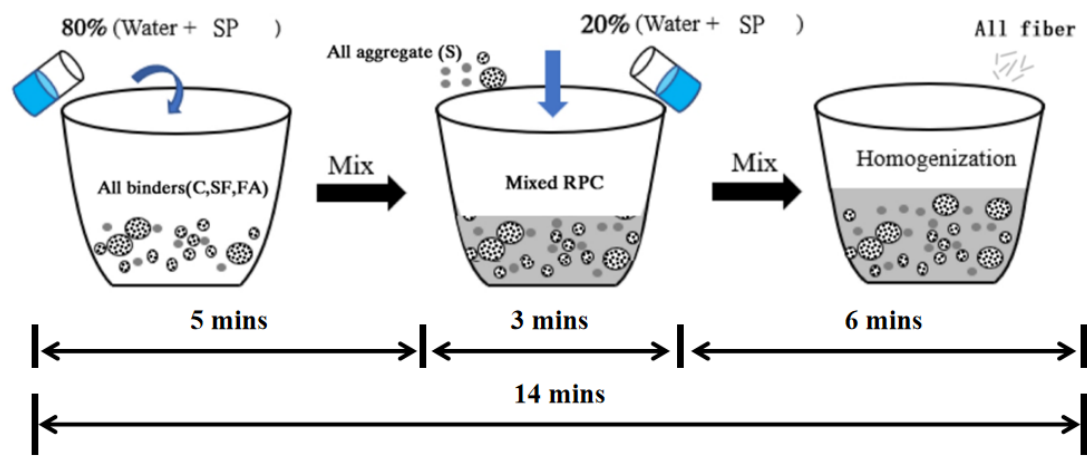
A mix proportion of RPC reported in a study [18] of RPC with cement partially replaced by FA of 0%, 10%, 15%, 20%, and 25% by weight was selected for this part. The selected proportion is the one with 15% FA that can give 3-day, 7-day, and 28-day compressive strength of 81, 106, and 147 MPa, respectively, and 28-day splitting tensile strength of 18.8 MPa. However, the original proportion, with SP of  $18.7 \text{ kg/m}^3$ , give a flow value of 130 mm less than the target value ( $200 \pm 10 \text{ mm}$ ) in this study. Therefore, the required amount of SP was determined to meet the set flow value and the final mix proportion used is in Table 6, that has a flow value of 198 mm.

Table 6. Compositions of RPC for Part I ( $\text{kg/m}^3$ ).

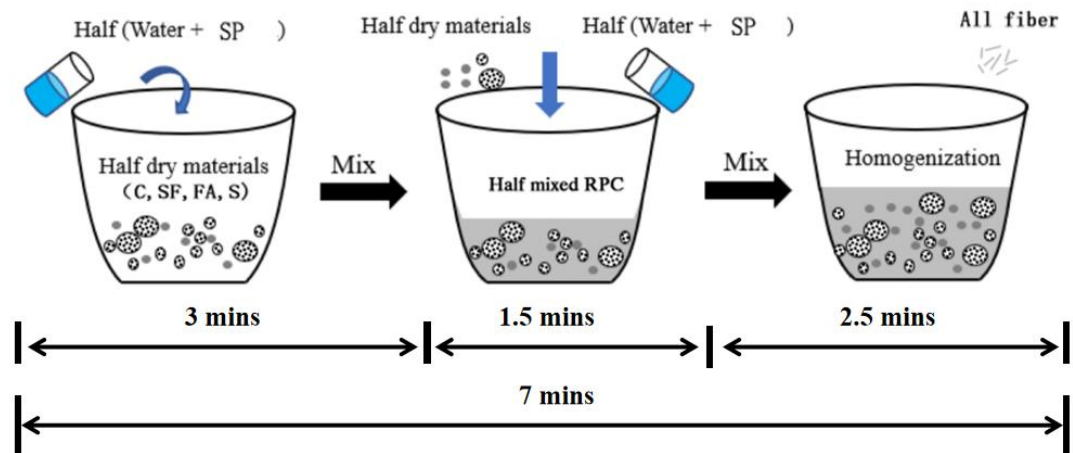
Material	Weight	Remark
Cement (C)	795	85% of C+FA
Fly Ash (FA)	140	15% of C+FA
Graded Sand (GS)	1028.5	$\text{GS}/(\text{C}+\text{FA}) = 1.1$
Silica Fume (SF)	187	$\text{SF}/(\text{C}+\text{FA}) = 0.20$
Superplasticizer (SP)	50	$\text{SP}/(\text{C}+\text{FA}) = 0.05$
Water (W)	215	$\text{W}/(\text{C}+\text{FA}) = 0.23$
Steel Fiber (STF)	233.8	$\text{STF}/(\text{C}+\text{FA}) = 0.25$

### 3.3 Mixing Techniques Investigated

This study employed two mixing methods, as illustrated in Figure 12, to investigate the effects of different techniques at mixing temperatures of 25°C and 40°C, using two types of steel fiber (single-size and mixed-size). The first method was the single-batching approach, commonly used for RPC mixing. The second method, a double-batching approach introduced by [15], employs a multi-step process designed to reduce mixing torque. For simplicity, more complex methods, such as triple-batching and other multi-step processes, were excluded from consideration.



(a) Single-batching method



(b) Double-batching method.

Figure 12. Single- and double- batching methods (modified from [15]).

#### 3.3.1 Single-Batching Method

Single batch mixing is the traditional method of concrete mixing and the following steps were used in this study:

Step 1: Mix all binders (C, SF, and FA). Then add 80% of the premixed liquid (W and SP). Stir until homogenized

Step 2: Add all aggregate (S) along with the remaining 20% of the premixed liquid (W and SP) then continue mixing until homogenized.

Step 3: Add all fibers (STF) for the final mixing stage until homogenized.

### 3.3.2 Double-Batching Method

The double batch mixing method is a new mixing method with the following main steps:

Step 1: Mix all binders (C, SF, and FA) with all aggregate (S) as show in Figure 13. Then take half of the mixed binder and aggregate and add half of the premixed liquid (W and SP) and stir until homogenized.



Figure 13. Mixing all binders and sand in a tray.

Step 2: Add the remaining half of the mixed binder and aggregate, along with the remaining half of the premixed liquid and stir until homogenized.

Step 3: Add all STF at the end of the final mixing stage until well blended. As show in Figure 14.



Figure 14. Adding steel fiber and continue mixing.



### 3.4 Specimen Preparation and Tests for Part I

A 5-litre standard mixer, generally used for conventional mortar, from MD Supply Co. Ltd., Thailand, was used for both mixing processes. At the end of each mixing process, a flow test in accordance with ASTM C1437-01 was conducted as illustrated in Figure 16.



Figure 15. The 5 litre standard mixer from MD Supply Ltd.



Figure 16. Flow testing.

Test specimens for 7-day and 28-day compressive strength according to ASTM C109 were prepared at temperature of 25°C, divided into three groups: Mix S-M-15FA-100GS served as the control mix, using the single-batching method with mixed-size steel fibers, 15% FA, and 100% GS; Mix D-M-15FA-100GS, using the double-batching method with mixed-size steel fibers, 15% FA, and 100% GS; and Mix D-S-15FA-100GS, using the double-batching method with single-size steel fibers, 15% FA, and 100% GS. The specimens were cast into steel cube molds with dimensions of 50 x 50 x 50 mm. All samples were wrapped in plastic sheeting to prevent moisture loss. After one day, the samples were removed from the molds and then cured in water until the day of the compression test, as shown in Figure 17.

The effects of mixing temperature were investigated only on flow of RPC.



Figure 17. Specimen preparation for Part I.

## Part II: Mechanical Properties of RPC Containing Fly Ash

### 3.5 Experimental Program for Part II

In order to investigate the mechanical properties of RPC containing fly ash using the appropriate mixing technique that is the double-batching method as discussed in Chapter 4, the experimental program was designed as showed in Table 7.

Fly ash was adopted to partially replace cement at 15% and 45% by weight. The 45% FA was selected as to study RPC with high amount of fly ash and to be more environmentally friendly. For the 15% FA was considered as explained in Part I. Moreover, to reduce unit cost of RPC, in this part sand used in every mixture was a combination of 30% graded river sand (GS) and 70% natural river sand (NS).

The mechanical properties evaluated were 3-day and 28-day compressive strengths, 28-day splitting tensile strength, and 28-day flexural strength.

Table 7. Experimental program for Part II.

Mix ID	Sand	Test	Standard	Specimen size	No.-Spec.
D-M-15FA-30 GS70NS	0.3GS +0.7NS	3d comp.	ASTM C39	100×200mm cylinder	4
		28d comp.			4
		28d splitting-tens.	ASTM C496	75×75×280mm prisms	4
		28d flex.			4
D-M-45FA-3 0GS70NS		3d comp.	ASTM C39	100×200mm cylinder	4
		28d comp.			4
		28d splitting-tens.	ASTM C496	75×75×280mm prisms	4
		28d flex.			4

Remark: D = Double-batching method; M=Mixed-size fibers; 15FA= 15% FA by weight of cement and fly ash; NS = Natural river sand; GS = Graded river sand.

### 3.6 Mix Proportions for Part II

As the mixing method was changed from single-batching method to double-batching method and sand used for this part was a combination of 30% graded river sand (GS) and 70% natural river sand (NS) which are different from the Part I, the amount of SP required for a target flow of  $250 \pm 10$  mm was, therefore, necessary to be determined again. The obtained SP and mix propositions for this part are concluded in Table 8. It can be observed that the amount of SP required for RPC with 15% FA in the Part II ( $30 \text{ kg/m}^3$ ) is less than that in the Part I ( $50 \text{ kg/m}^3$ ). This is a result of applying the double-batching method.

Table 8. Compositions of RPC for Part II ( $\text{kg/m}^3$ ).

Material	Mix	
	D-M-15FA-30GS70NS	D-M-45FA-30GS70NS
Cement (C)	795	514
Fly Ash (FA)	140	421
Natural Sand (NS)		720
Graded Sand (GS)		308
Silica Fume (SF)		187
Superplasticizer (SP)	30	60
Water (W)		215
Steel Fiber (STF):		233.8
Mixed-Size Flow (mm)	260	241

### 3.7 Specimen Preparation for Part II

All mixed were operated at room temperature using a 20-litre standard mixer, from Bosson Ltd., Thailand. Subsequent to the flow test, the freshly mixed RPC was poured into designated molds to produce specimens for each test. The molds were then covered with a plastic sheet to prevent the specimens from drying out. The specimens were left in the molds for 24 hours to allow the RPC to set as shown in Figure 19. The specimens were taken out of the molds and left to cure in tap water until testing date as shown in Figure 20.





Figure 18. The 20 litre standard mixer from Bosson Ltd in Thailand.



Figure 19. Example of Specimen preparing for Part II.



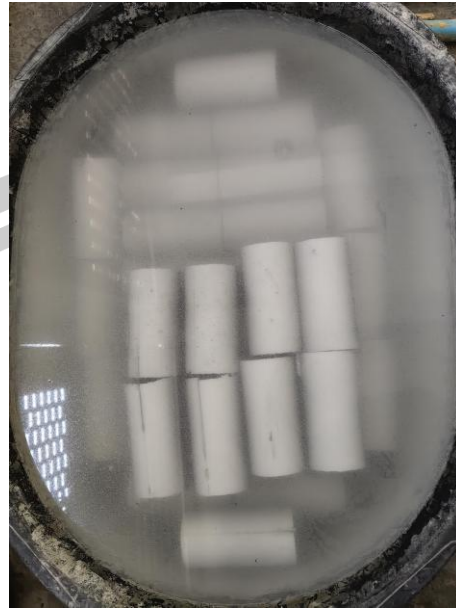


Figure 20 . Specimen curing (Part II).

### 3.8 Testing of Hardened RPC

#### 3.8.1 Compressive Strength Test

To determine the compressive strength of RPC in the Part I, each cube specimen of 50 mm x 50 mm x 50 mm was tested according to ASTM C109. And in the Part II, each cylinder specimen with diameter of 100 mm and height of 200 mm was tested as per ASTM C39.

In testing, the specimen was placed in the Universal Testing Machine (UTM) at the center of the actuator as shown in Figure 21. The test was then operated until the sample failed and the results were recorded. The compressive strength can be calculated using Eq. (3.1).

$$f_c' = \frac{P}{A} \quad (3.1)$$

where

$f_c'$  is compressive strength (MPa)

$P$  is the maximum force on the sample (N)

$A$  is the compressive cross-sectional area (mm<sup>2</sup>)



(a) ASTM C109



(b) ASTM C39

Figure 21. Compression test according to: (a) ASTM C109 and (b) ASTM C39.

### 3.8.2 Splitting Tensile Strength Test

The splitting tensile strength of RPC was tested according to ASTM C496 using a cylinder with diameter of 100 mm and height of 200 mm as shown in Figure 22. To receive the transmitted pressure, a 3 mm thick piece of plywood is placed at the top and bottom of the sample. The splitting tensile strength can be calculated using Eq. (3.2).



$$f_t = \frac{2P}{\pi LD} \quad (3.2)$$

where

$f_t$  is splitting tensile strength (MPa)

$P$  is the maximum force on the sample (N)

$L$  is the length of the cylindrical concrete sample (mm)

$D$  is the diameter of the concrete sample (mm)

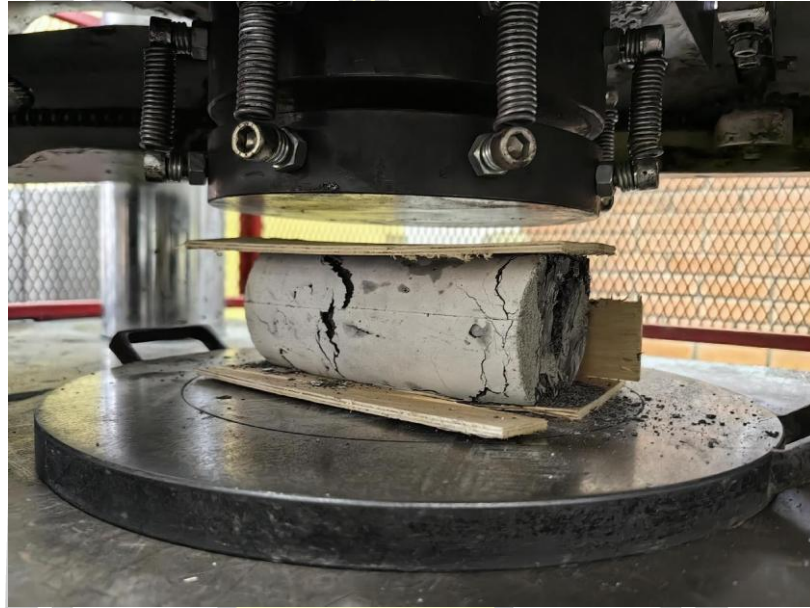


Figure 22. Splitting tensile strength test according to ASTM C496.

### 3.8.3 Flexural Strength Test

The flexural strength of RPC was tested according to ASTM C1609 using a prism with dimensions of 75 mm x 75 mm x 280 mm as shown in Figure 23. The flexural strength can be calculated using Eq. (3.3).

$$f_f = \frac{PL}{bd^2} \quad (3.3)$$

where

$f_f$  is flexural strength (MPa).

$P$  is the maximum force on the sample (N).

$L$  is the length of the rectangular concrete specimen (mm).

$b$  is the average width of the specimen at the fracture, orientation at test (mm).

$d$  is the average depth of the specimen, orientation at test (mm).

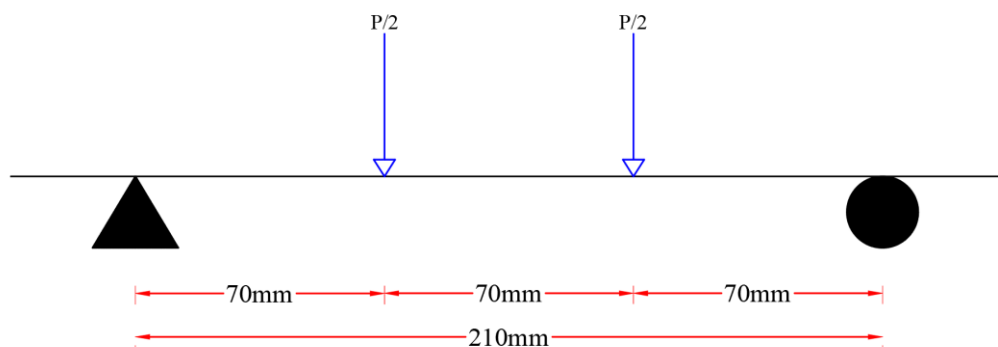
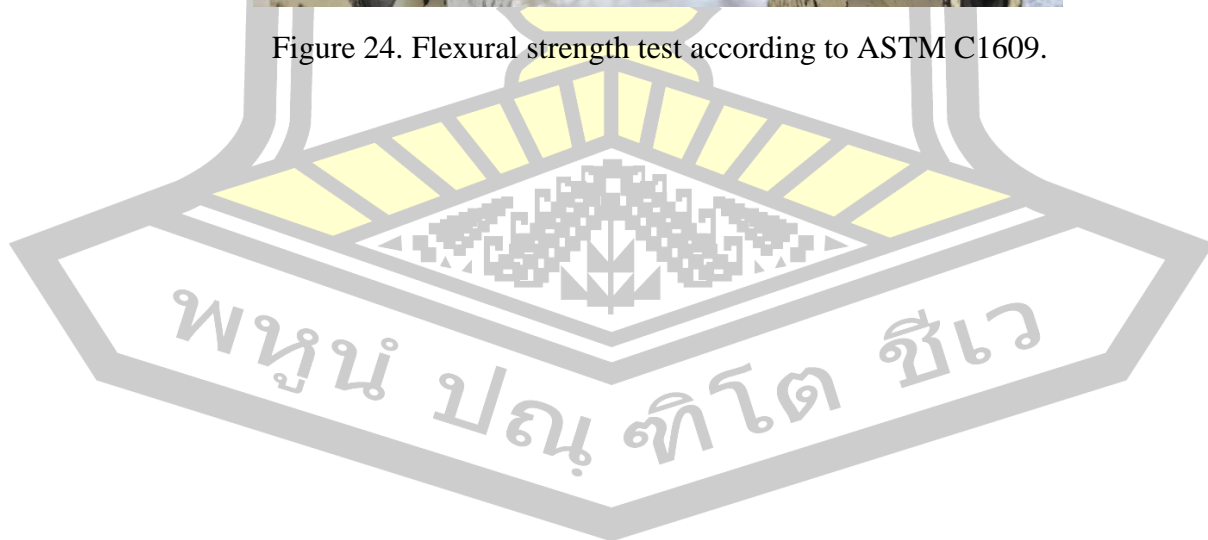


Figure 23. Two-point Flexural Strength testing.



Figure 24. Flexural strength test according to ASTM C1609.



## Chapter 4

### Test Results and Analysis

In this chapter, the test results of both parts are presented including (1) Part I, the results of studying the effects of mixing techniques on the properties of reactive powder concrete (RPC) containing fly ash to consider a suitable mixing technique and (2) Part II, the results of investigating the mechanical properties of RPC containing fly ash using the appropriate mixing technique.

#### 4.1 Part I: Effects of Mixing Techniques

In this part, the effects of mixing methods in terms of flow value, 7-day compressive strength, and 28-day compressive strength; the effects of types of steel fiber on the best mixing method; and the effects of mixing temperatures on flow value of RPC are presented and discussed.

##### 4.1.1 Effects of Mixing Methods

Table 9 presents a summary of the results obtained from the flow properties and compression strength tests conducted on the RPC at temperature of 25°C. The values for compression strength were calculated as an average based on measurements from four specimens, thereby ensuring the accuracy of the data. A comparison of the test results for Mix S-M-15FA-100GS (using the single-batch mixing method) with those for Mix D-M-15FA-100GS (using the double-batch mixing method) allows the influence of the preparation process on the material properties to be observed. The utilization of the double-batch mixing method has been observed to markedly enhance the flow properties of the RPC in comparison to the single-batch mixing method, with a 21.7% increase in flow values. This observed enhancement in flow properties may be attributed to the fact that the double-batch mixing method effectively reduces the peak mixing torque during the mixing process as reported by [15], thus promoting the homogeneous dispersion of the material with better flow properties. In other words, the double-batch method necessitates less energy to achieve uniform mixing. This finding is consistent with the trend reported by [15], which showed a 3.5% increase in flow value. Nevertheless, as illustrated in Figure 25, the double-batching method exerted a considerable influence on the 28-day compressive strength, which exhibited a 7.6% increase relative to the single-batch method. The 7-day compressive strength exhibited no significant difference between the two methods. This result differs from the finding in [15], which reported no significant effect on compressive strength at any age. The greater increase in both flow value and 28-day compressive strength observed in this study may be due to the influence of the rounded particles in the FA and SF, as shown in Figure 10(b) and Figure 11(c), respectively. Figure 26 and Figure 27 present the specimens with the single-batching method (before and after the compression tests) and with the double-batching method, respectively.

Table 9. Results of RPC mixing at a constant temperature of 25°C.

Mix ID	Mixing Method	Steel Fiber Type	Flow Value (mm)	Compressive strength			
				7-day		28-day	
				Strength	COV	Strength	COV
S-M-15FA-100GS	Single-Batch	Mixed size	198	89.4 MPa	8.7%	123.2 MPa	12.2%
D-M-15FA-100GS	Double-Batch	Mixed size	241	88.3 MPa	2.7%	132.6 MPa	8.6%
D-S-15FA-100GS	Double-Batch	Single size	257	88.5 MPa	7.7%	118.4 MPa	10.4%

Remark: COV is coefficient of variation.

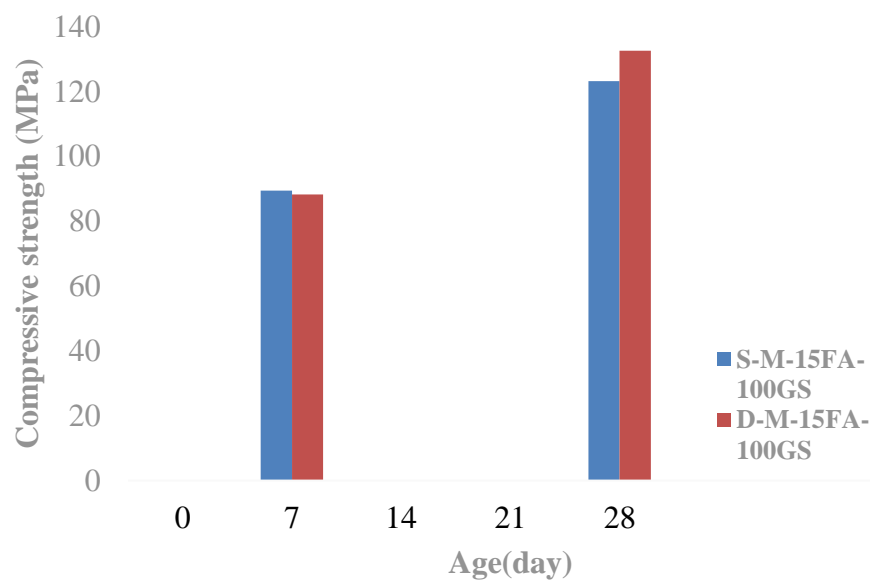
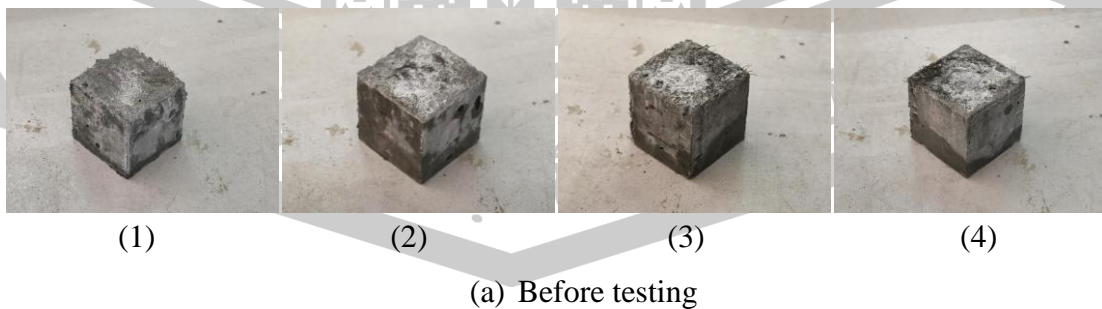


Figure 25. Effect of mixing method on RPC compressive strength.





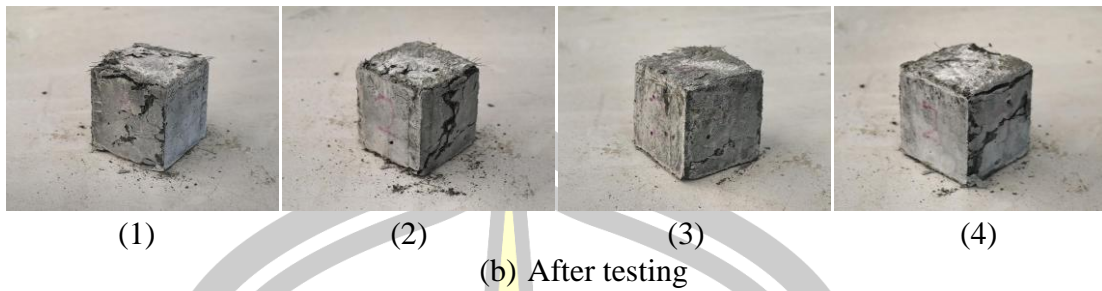


Figure 26. Samples with single-batching method for compression test: (a) before testing and (b) after testing

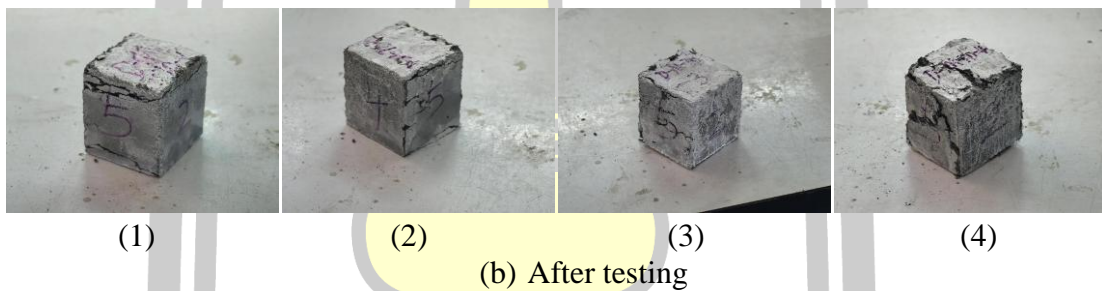
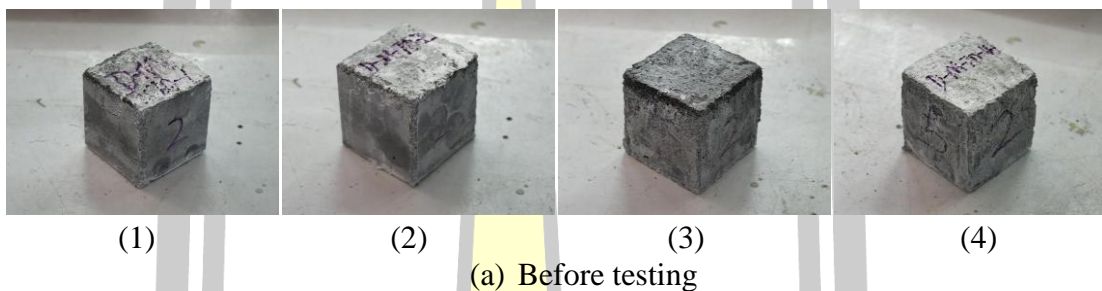


Figure 27. Samples with double-batching method for compression test: (a) before testing and (b) after testing

#### 4.1.2 Effects of Type of Steel Fiber

The previous section outlines the advantages of the double-batching method on the workability and 28-day compressive strength of RPC incorporating mixed-size steel fibers. In this section, the influence of steel fiber type on the double-batching method is examined by comparing the results of Mix D-M-15FA-100GS, which employed mixed-size fibers with an average aspect ratio of 56, and Mix D-S-15FA-100GS, which utilized single-size fibers with a constant aspect ratio of 59.

According to the data presented in Table 9, the flow value of RPC with single-size fiber is 6.6% higher than that with mixed-size fiber due to its constant aspect ratio of 59, which highlights the positive effect of fiber size consistency on flowability. However, when comparing the contributions of the two mixtures to compressive strength, the situation is different. As clearly shown in Figure 28, the compressive strength of the two mixtures at 7 days is almost the same. It is worth noting that although the single-size fiber performs well in flowability, they have an adverse effect on the 28-day compressive strength, which is 10.7% lower than the

compressive strength of mixed-size fiber. The reason for this result may be that the smaller the aspect ratio, the more conducive it is to improve the compressive strength. Figure 29 and Figure 30 present the specimens with mixed-size steel fibers (before and after the compression tests) and with single-size steel fibers, respectively.

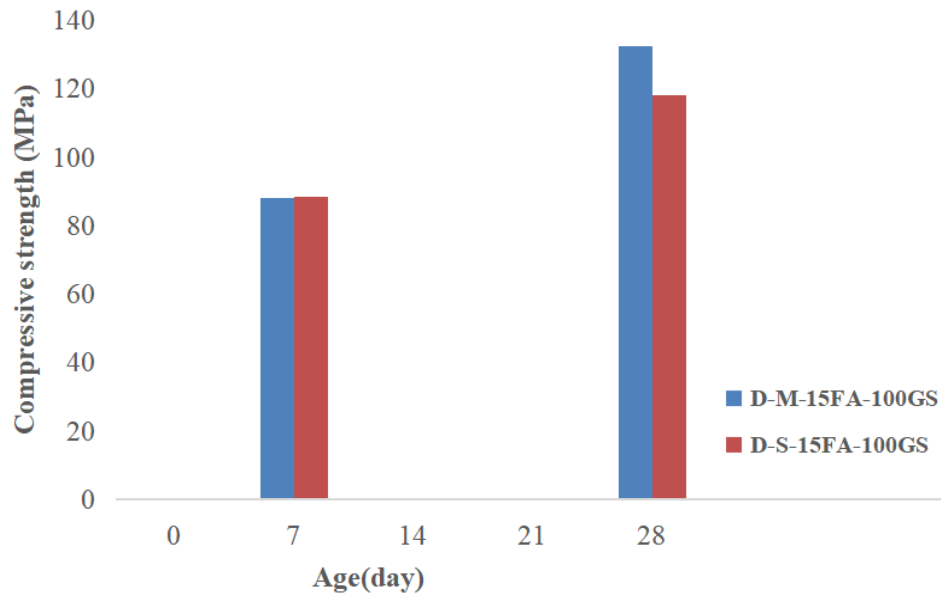


Figure 28. Effects of type of steel fiber on RPC compressive strength.

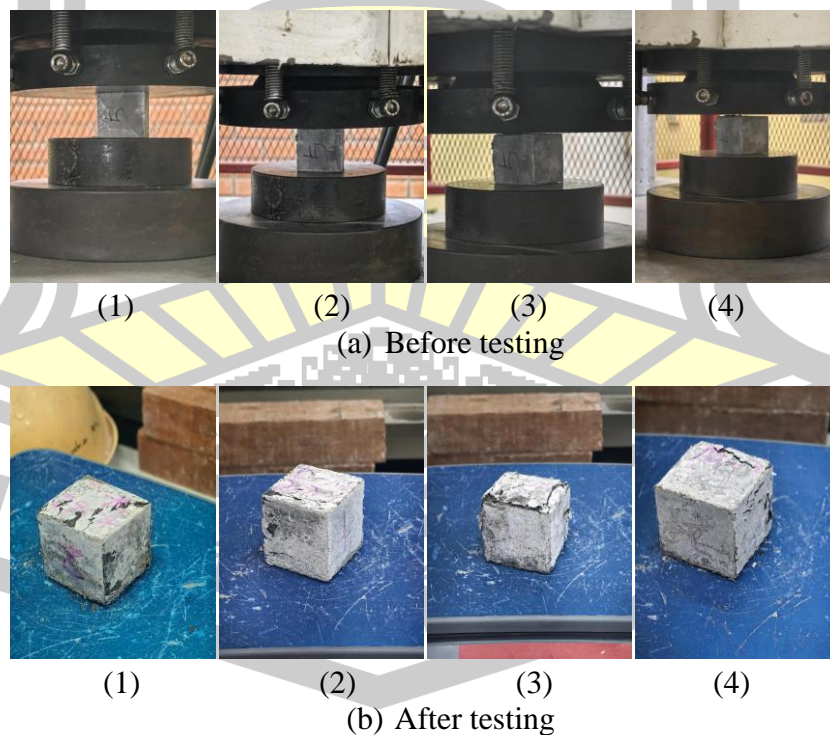


Figure 29. Samples with mixed-size fibers for compression test: (a) before testing and (b) after testing



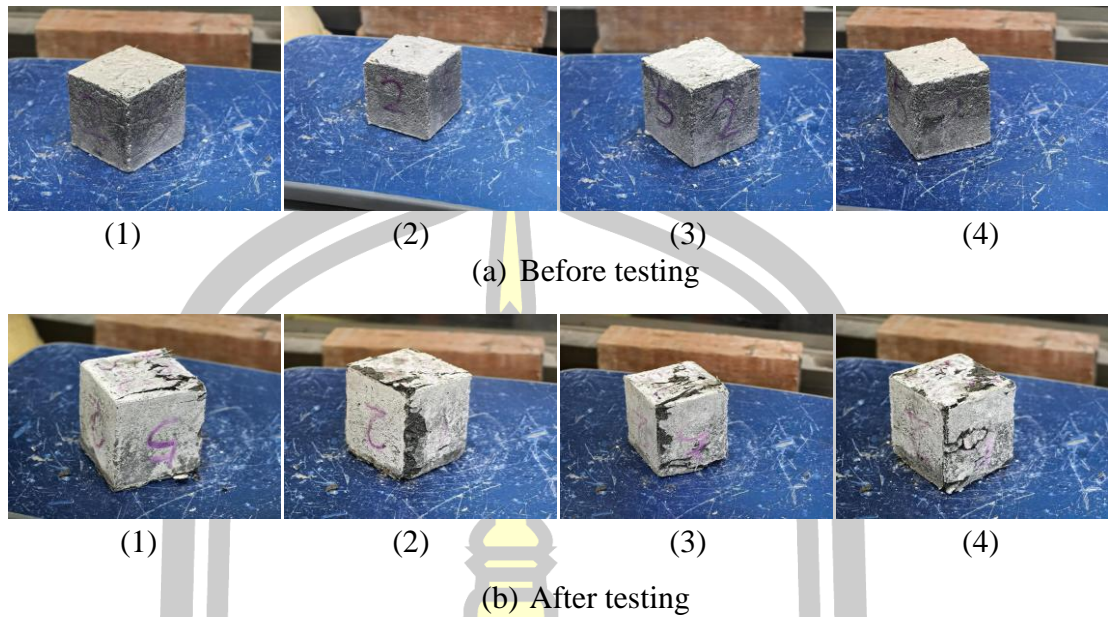


Figure 30. Samples with single-size fibers for compression test: (a) before testing and (b) after testing

#### 4.1.3 Effects of Mixing Temperature on Flow Value of RPC

Furthermore, in order to gain a deeper understanding of the impact of mixing temperature on the flowability of RPC using double-batching method, the control mix (S-M-15FA-100GS) with SP value set at  $45 \text{ kg/m}^3$  was utilized, with mixing conducted at temperatures of  $25^\circ\text{C}$  and  $40^\circ\text{C}$ . The selected temperatures aimed to simulate RPC production under different seasonal conditions. The  $25^\circ\text{C}$  setting was for mixing in an air-conditioned room and the  $40^\circ\text{C}$  was for mixing at outdoor temperatures during the Thai summer season.

The results of the flow value test are shown in Table 10. A comparison of the test data presented reveals a discernible trend. As the temperature of the mixture increases, the workability values exhibit a declining trend. In particular, when the ambient temperature was elevated from a baseline of  $25^\circ\text{C}$  to a higher temperature of  $40^\circ\text{C}$ , there was a notable reduction in the flow value of approximately 5.9%, which can be attributed to the accelerated evaporation of water from the mixture at elevated temperatures. This finding confirms that mixing temperature is also one of the key factors affecting the flow properties of materials.

Table 10. Flow values of RPC with different mixing temperatures.

Mix	SP ( $\text{kg/m}^3$ )	Mixing Temperature ( $^\circ\text{C}$ )	Flow Value (mm)
S-M-15FA-100GS	45	25	187
		40	176

## 4.2 Part II: Mechanical Properties of RPC Containing Fly Ash

From the first part, it was found that the double-batching method is better than the single-batching method. In this part, the mechanical properties of RPC, containing fly ash (15% and 45%) and a combination of graded and natural river sand, using the double-batching method are presented and discussed. The mechanical properties investigated were 7-day and 28-day compressive strength, 28-day splitting tensile strength, and 28-day flexural strength. The density of RPC is also reported. In addition, the result of a preliminary study of compressive strength at an elevated temperature is also mentioned.

### 4.2.1 Density

The 28-day density of RPC samples with different proportions of fly ash was determined. The test results are shown in Table 11. The average density was obtained from all samples used in the tests of the mechanical properties.

Table 11. Density for RPC with different fly ash contents

Mix ID	FA	Average Density (kg/m <sup>3</sup> )
D-M-15FA-30GS70NS	15%	2,324
D-M-45FA-30GS70NS	45%	2,225

The results of the density tests of RPC containing fly ash showed that the average density of RPC containing 45%FA is lower than that of RPC containing 15%FA about 4.3%. This may be due to the fact that fly ash (S.G.=2.70) has a lower specific gravity (S.G.) than cement (S.G.=3.15) and, due to its lightweight nature, occupies more volume in the mix. Also, the incorporation of more fly ash can lead to an increase in porosity within the concrete at a given water-cement ratio. These tiny pores can lead to a decrease in the density of the concrete.

### 4.2.2 Compressive Strength

Compressive strength was tested according to ASTM C39 using 10\*20 cm cylindrical samples. Samples were tested at 3 and 28 days of age and the test results are detailed in Table 12. The result of each group of tested samples was averaged from 4 samples and the average compressive strength results obtained after 3 days were 65.69 MPa for RPC with 15% FA and 32.6 MPa for RPC with 45% FA. The average compressive strength results obtained after 28 days were 121.2 MPa for RPC with 15% FA and 109.4 MPa for RPC with 45% FA. Comparison of test results is shown in Figure 31.

Table 12. Compressive strength of RPC with 15%FA and 45%FA using double-batching method.

Mix ID	FA	SP (kg/m <sup>3</sup> )	Flow Value (mm)	Compressive strength			
				3-day		28-day	
				Strength	COV	Strength	COV
D-M-15FA-30GS70NS	15%	30	260	65.7 MPa	3.7%	121.2 MPa	4.55%
D-M-45FA-30GS70NS	45%	60	241	32.6 MPa	6.0%	109.4 MPa	2.92%

Remark: COV is coefficient of variation.

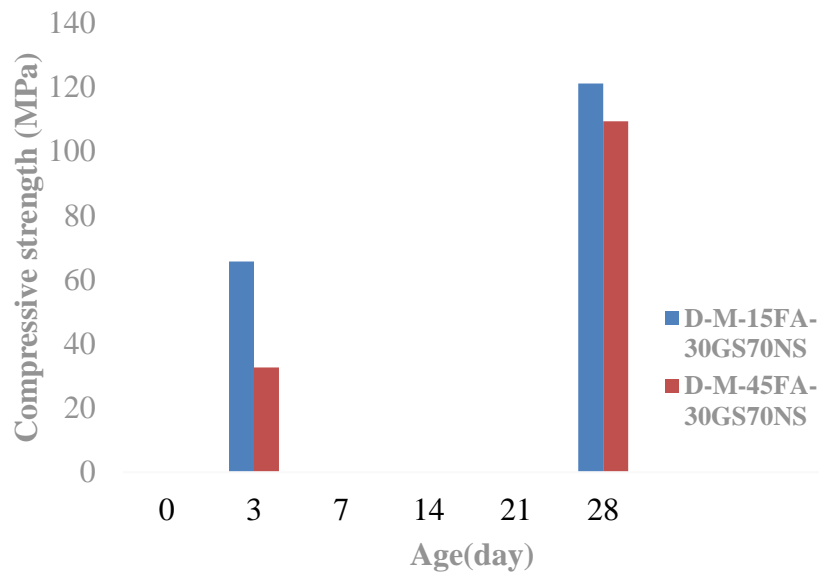


Figure 31. Comparison of 3-day and 28-day compressive strength.

In the 3-day compressive strength test, it was observed that the compressive strength of concrete specimens with different fly ash contents was significantly different, and the compressive strength of 45%FA-RPC specimens was about 50.38% lower than that of 15%FA-RPC specimens. This indicates that the mixes with lower fly ash content had better early strength performance at lower superplasticizer content. This may be due to the fact that cement hydration reaction is dominant, and the 15% FA mixture with higher cement content produces more hydration products, such as C-S-H gel, than the 45% FA mixture, thus providing higher early strength. The 45% FA mixture has a lower cement content and a slower early hydration reaction, resulting in a larger strength difference at 3 days. At the same time, while the higher superplasticizer content improved the flow of the specimens, it may have also affected the early compressive strength growth of the RPC.

In the 28-day test, it was found that the compressive strength of specimens with different mix ratios also differed. The specimens with 45% FA-RPC still showed a

compressive strength lower than that of the specimens with 45% FA-RPC, but the difference was less than the 3-day compressive strength, and its strength decreased by about 9.74%. This may be because the pozzolanic reaction of fly ash began to take effect over time. The silicates in the fly ash reacted with the calcium hydroxide produced by cement hydration to produce more C-S-H gel, which made up for the lack of early strength and narrowed the strength gap with the 15% FA mixture. In addition, the high content of fly ash further filled the pores in the concrete, improving the density and durability of the material. Therefore, although the early strength of 45% FA was lower, its microstructure was gradually improved, gradually narrowing the gap in early strength with the 15% FA mixture.

In general, the early compressive strength decreased with the increase in the percentage of fly ash content. In RPC, the pozzolanic reaction is the reason for the subsequent increase in strength. As time goes by, the generated C-S-H gel helps the adhesion of cement and aggregate and improves the strength of aggregate. It is expected to reach its maximum level of compressive strength after 28 days.

#### 4.2.3 Split Tensile Strength

The splitting tensile strength was tested according to ASTM C496 using 10\*20 cm cylindrical samples. The samples were tested at 28 days of age. The test results are shown in Table 13. The result of each set of tested samples was averaged from 4 samples. As shown in Figure 32, the average splitting tensile strength at 28 days is 18.6 MPa for D-M-15FA-30GS70NS, while the strength of 45%FA-RPC is 19.9 MPa.

Table 13. Splitting tensile strength of RPC with 15%FA and 45%FA using double-batching method.

Mix ID	FA	SP (kg/m <sup>3</sup> )	Flow Value (mm)	28-day splitting tensile strength	
				Strength	COV
D-M-15FA-30GS70NS	15%	30	260	18.6 MPa	7.1%
D-M-45FA-30GS70NS	45%	60	241	19.9 MPa	11.8%

Remark: COV is coefficient of variation.

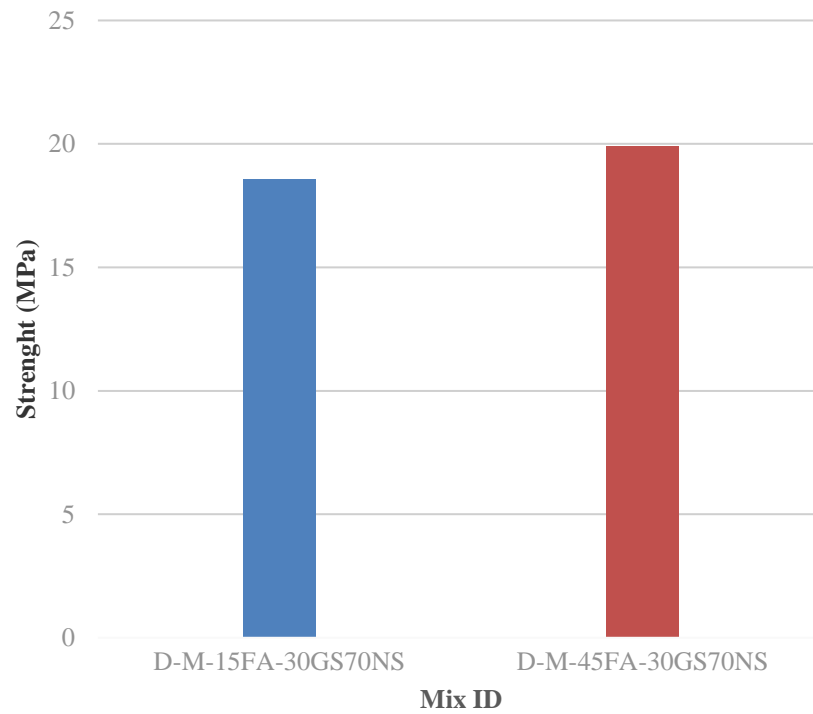


Figure 32. 28 days splitting tensile strength.

The results show that the splitting tensile strength of 45%FA-RPC was higher than that of 15%FA-RPC, with a strength increase of about 7.0%. This result shows that a higher fly ash content effectively improves the tensile properties of concrete over a long period of time, which is closely related to the pozzolanic reaction of fly ash in the later stage. At 28 days, RPC with a higher fly ash content of 45% generates more C-S-H gel through the pozzolanic reaction, further filling the pores and improving the compactness and tensile properties of concrete. At the same time, since a higher fly ash content improves the microstructure of concrete and reduces the porosity, the material can disperse stress more evenly when subjected to tension, reducing the phenomenon of tensile stress concentration [44, 46].

Although 45% fly ash replaces part of the cement, through the later chemical reaction, the fly ash effectively makes up for the lack of cement hydration products, thereby enhancing the tensile properties.

Table 14 illustrates the split tensile and compressive strength results and their ratio relationship formulae from this study and compares them with the relevant literature. The formula for the relationship between compressive strength and flexural strength of ACI 318-99 is  $0.56 f_c^{0.5}$  with a coefficient of difference of about 70%. The formula for the relationship between compressive strength and flexural strength in the study of Nihal et al. is  $(0.387 f_c^{-0.37}) f_c'$  with a coefficient of difference of about 58%. The formula for the relationship between the ratio of compressive strength to flexural strength obtained in the present study is  $0.167 f_c'$  with a coefficient of difference of about 8%.



Table 14. The relationship between the ratio of splitting tensile strength to compressive strength in this study and related literature.

Test Results		Formulae for Prediction Splitting Tensile Strength						
Splitting	Comp.	ACI 318-99 <sup>[53]</sup>		Nihal et al.(2006) <sup>[54]</sup>		This study		
$f_t$ (MPa)	$f_c'$ (MPa)	$0.56 f_c'^{0.5}$ (MPa)	Diff. (%)	$(0.387 f_c'^{0.37}) f_c'$ (MPa)	Diff. (%)	$0.167 f_c'$ (MPa)	Diff. (%)	
D-M-15FA-30GS70NS	18.6	121.2	6.2	-66.9	7.9	-57.3	20.2	8.8
D-M-45FA-30GS70NS	19.9	109.4	5.9	-70.6	8.3	-58.1	18.3	-8.2

#### 4.2.4 Flexural Strength

The flexural strength test was conducted according to ASTM C1609 using 7.5\*7.5\*28 cm rectangular specimens. The specimens were tested at 28 days. The test results are shown in Table 15. The result for each set of tested specimens was averaged from 4 specimens. As shown in Figure 33, the average flexural strength at 28 days was 22.4 MPa for D-M-15FA-30GS70NS, while the strength of D-M-45FA-30GS70NS was 24.2 MPa.

Table 15. Flexural strength of RPC with 15%FA and 45%FA using double-batching method

Mix ID	FA	SP (kg/m <sup>3</sup> )	Flow Value (mm)	28-day flexural strength	
				Strength	COV
D-M-15FA-30GS70NS	15%	30	260	22.4 MPa	16%
D-M-45FA-30GS70NS	45%	60	241	24.2MPa	13.8%



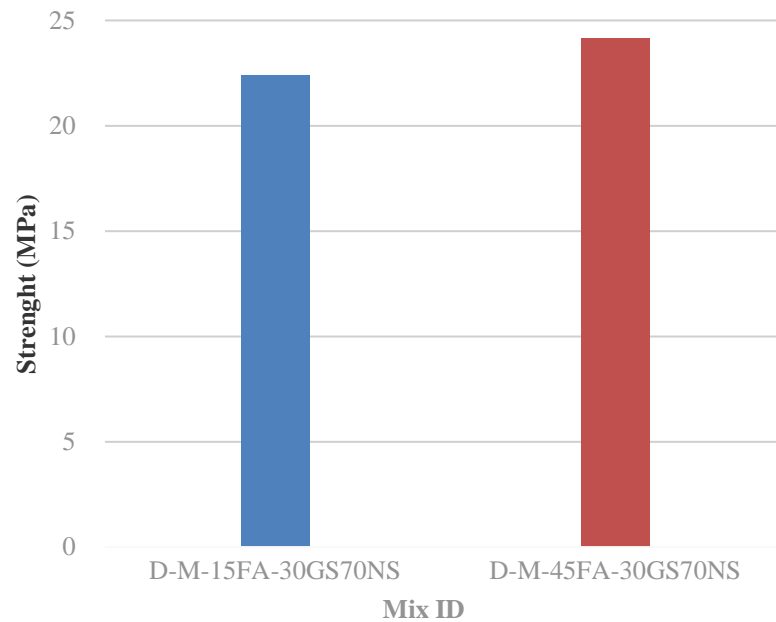


Figure 33. 28 days flexural strength.

The 28-day flexural strength results show that when a higher proportion of fly ash was used, RPC exhibited enhanced flexural properties at 28 days. The flexural strength of the specimens with 45%FA-RPC increased by about 8.0% compared to the specimens with 15%FA-RPC. This phenomenon may be attributed to the delayed impact of fly ash. The pozzolanic reaction of the RPC mixture with 45% fly ash becomes more pronounced at 28 days due to the elevated fly ash content, resulting in the generation of greater quantities of C-S-H gel. Furthermore, the bonding between the fiber and the matrix is enhanced. The elevated proportion of fly ash facilitates enhanced interfacial adhesion between the steel fiber and the cement matrix, thereby mitigating the propagation of fissures and consequently augmenting the flexural strength. This is related to the significant role of fiber in stress transfer. The higher fiber bonding force enables the material to better resist bending stress. Additionally, although the density of the 45%FA-RPC is slightly lower than that of the 15%FA-RPC, the internal microstructure of the material is optimized due to the filling effect of fly ash, resulting in a reduction in porosity and an enhanced overall flexural capacity. And it has been shown that W/C ratio is also one of the important factors affecting the flexural strength of concrete containing fly ash [57].

Table 16 lists the flexural strength and compressive strength results of this study and their ratio relationship formulas, and compares them with relevant literature. The formula for the relationship between the compressive and flexural strengths of ACI 318-08 is  $0.62 f_c^{0.5}$ , which is a coefficient of difference of approximately 70%. The formula for the value of the relationship between compressive and flexural strength in the study of Leemann and Hoffmann is  $0.11 f_c'$  and the coefficient of difference is about 45%. The relationship equation for the ratio between compressive strength and flexural strength obtained in this study is  $2.172 f_c^{0.5}$  with a coefficient of difference of about 6%.

Table 16. The relationship between the ratio of flexural strength to compressive strength in this study and related literature.

	Test Results		Formulae for Prediction Flexural Strength					
	Flex.	Comp.	ACI 318-08 <sup>[55]</sup>		Leemann & Hoffmann (2005) <sup>[56]</sup>		This study	
	$f_f$ (MPa)	$f_c'$ (MPa)	$0.62 f_c'^{0.5}$ (MPa)	Diff. (%)	$0.11 f_c'$ (MPa)	Diff. (%)	$2.172 f_c'^{0.5}$ (MPa)	Diff. (%)
D-M-1 5FA-3 0GS70 NS	22.4	121.2	6.8	-69.5	13.3	-40.5	23.9	6.8
D-M-4 5FA-3 0GS70 NS	24.2	109.4	6.5	-73.2	12.0	-50.3	22.7	-6.1

#### 4.2.5 Effects at High Temperatures

Meanwhile, a series of samples of D-M-15FA-30GS70NS and D-M-45FA-30GS70NS were prepared to evaluate their compressive strength after heat treatment at different high temperatures. To test the samples at high temperatures, the samples were first conditioned at room temperature, and then placed in an oven at high temperatures for two hours after being heated to a specific temperature (400°C, 600°C, 800°C, or 1000°C). The samples were then removed from the oven, air-cooled at room temperature for 24 hours, and then tested for compressive strength. The temperature-time curves of the oven at different exposure temperatures are shown in Figure 34. The first test started with heating to 400°C. In the oven heating test, it was observed that when the temperature approached 400°C, the samples in the oven underwent violent explosive destruction, resulting in serious damage to the test oven, as shown in Figure 35, which shows the intensity of the explosion.

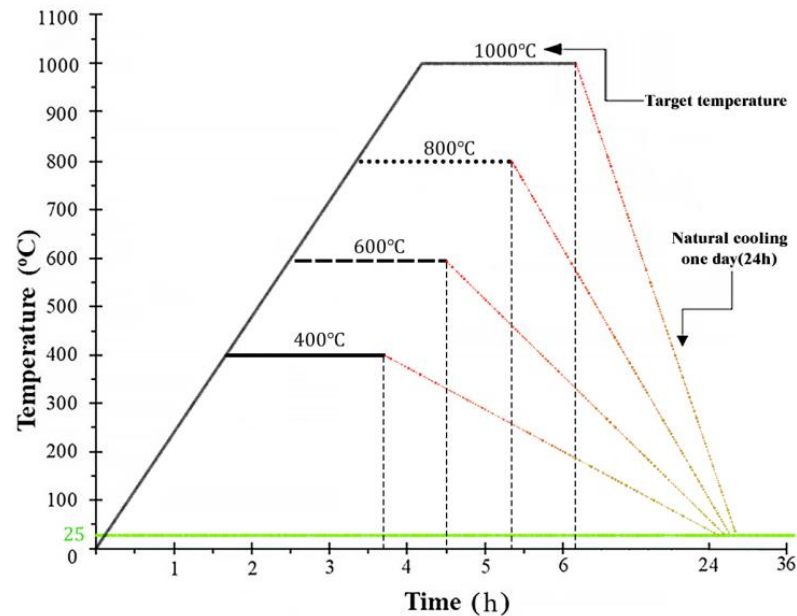


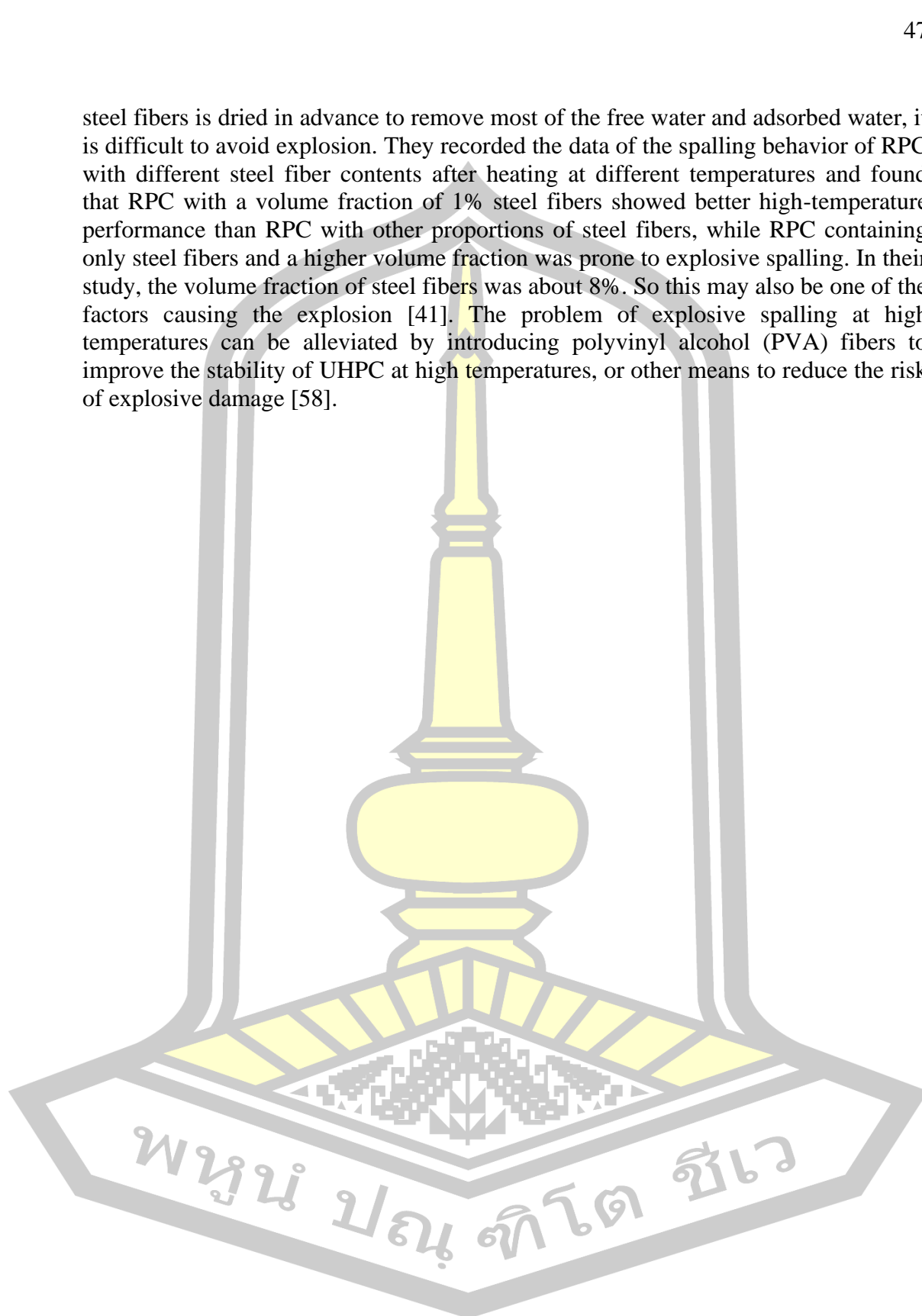
Figure 34. Temperature-time curves for different target temperatures using oven heating.



Figure 35. Explosive spalling of samples at high temperatures.

This phenomenon may be attributed to the small amount of free water in UHPC. Under high temperature, the internal water evaporates quickly and turns into water vapor, resulting in an uneven thermal gradient. At the same time, due to the extremely dense pore structure of UHPC and the strong bonding force between the fiber and the matrix, it is difficult for water vapor to escape effectively. As a result, the internal pressure of the concrete rises sharply. Once the pressure exceeds the bearing limit of the concrete, the specimen will explode and collapse [58]. In addition, the research results of Sanchayan et al. [41] also pointed out that even if the RPC containing only

steel fibers is dried in advance to remove most of the free water and adsorbed water, it is difficult to avoid explosion. They recorded the data of the spalling behavior of RPC with different steel fiber contents after heating at different temperatures and found that RPC with a volume fraction of 1% steel fibers showed better high-temperature performance than RPC with other proportions of steel fibers, while RPC containing only steel fibers and a higher volume fraction was prone to explosive spalling. In their study, the volume fraction of steel fibers was about 8%. So this may also be one of the factors causing the explosion [41]. The problem of explosive spalling at high temperatures can be alleviated by introducing polyvinyl alcohol (PVA) fibers to improve the stability of UHPC at high temperatures, or other means to reduce the risk of explosive damage [58].



# Chapter 5

## Conclusions

### 5.1 Part I: Effects of Mixing Techniques

#### 5.1.1 Mixing Methods

The utilization of the double-batch mixing method (241 mm flow) was observed to markedly enhance the flow properties of the RPC in comparison to the single-batch mixing method (198 mm flow), with a 21.7% increase in flow values. Moreover, the double-batching method (132.6 MPa) exerted a considerable influence on the 28-day compressive strength, which exhibited a 7.6% increase relative to the single-batch method (123.2 MPa). The 7-day compressive strength exhibited no significant difference between the two methods.

#### 5.1.2 Steel Fiber Types

The flow value of RPC with single-size fiber (257 mm flow) was 6.6% higher than that with mixed-size fiber (241 mm flow). While, the compressive strength of the two mixtures at 7 days was almost the same. However, the single-size fiber (118.4 MPa) had an adverse effect on the 28-day compressive strength, which was 10.7% lower than the compressive strength of mixed-size fiber (132.6 MPa).

#### 5.1.3 Mixing Temperature and Flow Value

As the temperature of the mixture increased, the workability values exhibited a declining trend. When the ambient temperature was elevated from a baseline of 25°C (187 mm flow) to a higher temperature of 40°C (176 mm flow), there was a notable reduction in the flow value of approximately 5.9%.

### 5.2 Part II: Mechanical Properties of RPC Containing Fly Ash

#### 5.2.1 Density

The average density of RPC containing 45%FA was lower than that of RPC containing 15%FA about 4.3%. The average density of RPC containing 45%FA and 15%FA was 2,225 kg/m<sup>3</sup> and 2,324 kg/m<sup>3</sup>, respectively.

#### 5.2.2 Compressive Strength at 3 and 28 Days

The 3-day compressive strength of 45%FA RPC (32.6 MPa) was about 50.38% lower than that of 15%FA RPC (65.7 MPa). The 28-day compressive strength of 45%FA RPC (109.4 MPa) was about 9.74% lower than that of 15%FA RPC (121.2 MPa).

#### 5.2.3 Splitting Tensile Strength

In contrast to the compressive strength, the 28-day splitting tensile strength of 45%FA-RPC was 7.0% higher than that of 15%FA-RPC. The 28-day splitting tensile strength of 45%FA RPC and 15%FA RPC was 19.9 MPa and 18.6 MPa, respectively.

This study found that the 28-day splitting tensile strength can be estimated from the 28-day compressive strength as  $0.167f_c'$ , with an error of less than 9%.

#### **5.2.4 Flexural Strength**

In contrast to the compressive strength, the 28-day flexural strength of 45%FA-RPC was 8.0% higher than that of 15%FA-RPC. The 28-day flexural strength of 45%FA RPC and 15%FA RPC was 24.2 MPa and 22.4 MPa, respectively.

This study found that the 28-day flexural strength can be estimated from the 28-day compressive strength as  $2.172f_c'^{0.5}$ , with an error of less than 7%.

#### **5.2.5 Performance at High Temperatures**

This study found that the RPC sample exhibited a sudden and violent failure at approximately 400°C. Therefore, the tests at higher temperatures were not considered.

### **5.3 Suggestion**

#### **5.3.1 Optimization of Fly Ash Content and Environmental Benefits**

For engineering structures that require long-term high strength and toughness, it is recommended to use RPC with a fly ash replacement ratio of 45%; for projects that require rapid construction and early strength, RPC with a fly ash replacement ratio of 15% is more appropriate. At the same time, high fly ash content not only improves the mechanical properties of RPC, but also significantly reduces the use of cement, reduces production costs and environmental impact, and thus can achieve economic and environmental benefits.

#### **5.3.2 Application Areas**

The simultaneous improvement of flexural strength and splitting tensile strength shows that D-M-45FA-30GS70NS performs well when subjected to stress in different directions. This means that the material performs well in applications with complex stress states (such as bridges, roads or other large-span structures). D-M-15FA-30GS70NS is more suitable for infrastructure construction projects with higher early strength requirements.

#### **5.3.3 Future Research**

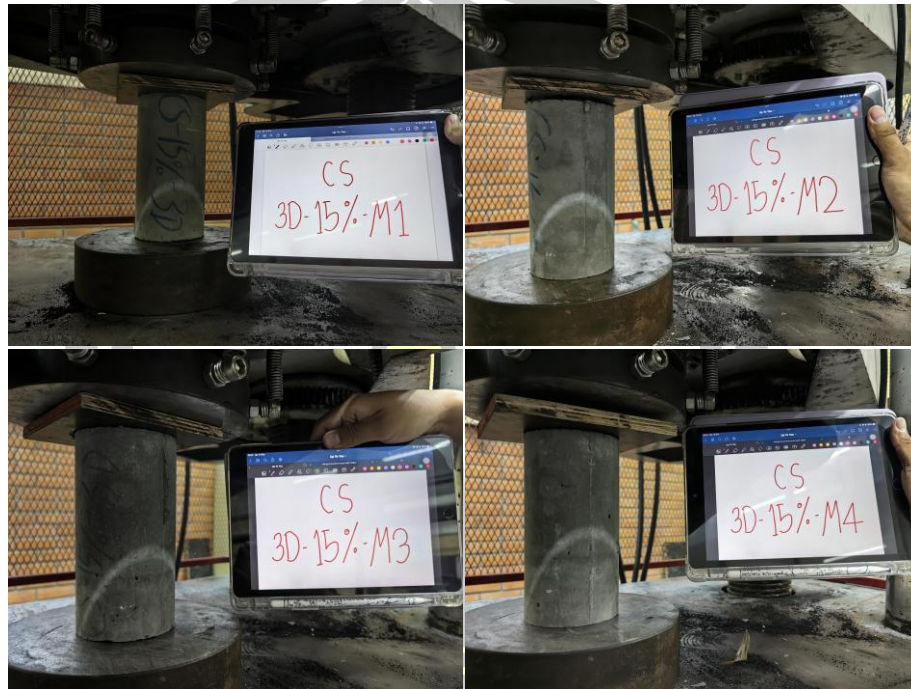
Although the use of 45% fly ash to replace cement has shown significant performance advantages, future research can further optimize the fly ash dosage and explore the mechanical properties and durability performance under higher dosages and longer curing cycles.

As RPC with steel fibers experiences sudden failure at around 400°C, future research on RPC with various types of fibers is needed.

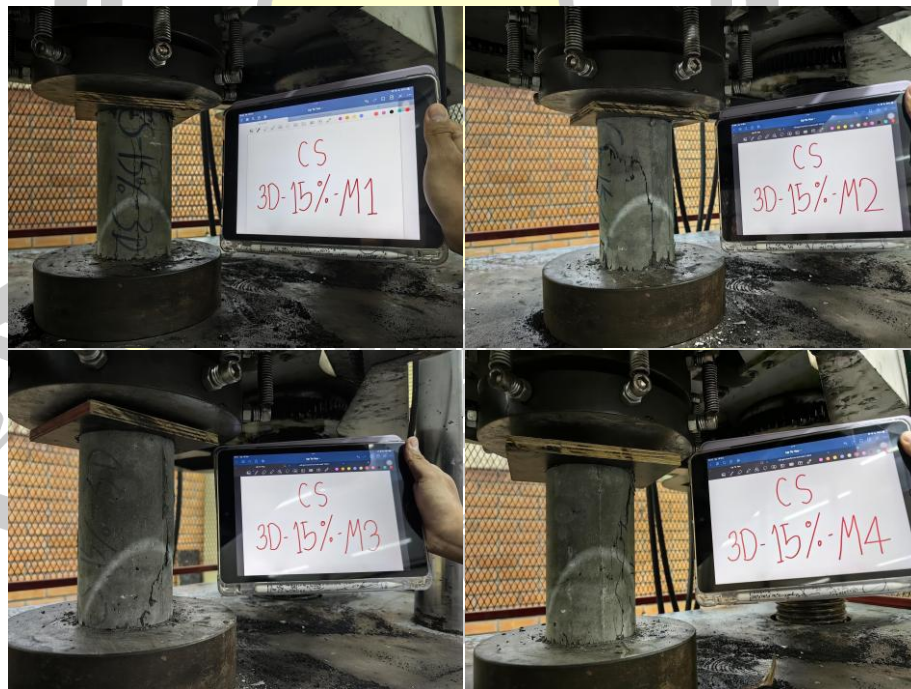


## Appendix A: Pictures of the Tests

### A1: Compression Strength Tests

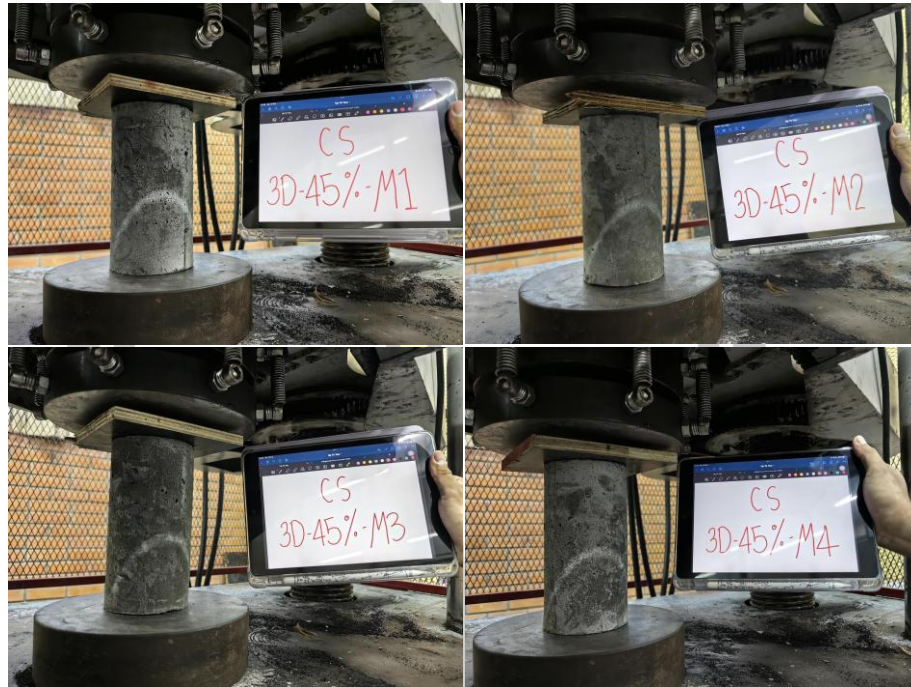


(a) Before testing



(b) After testing

Figure 36. D-M-15FA-30GS70NS samples for 3 days compressive strength testing:(a) before testing and (b) after testing



(a) Before testing



(b) After testing

Figure 37. D-M-45FA-30GS70NS samples for 3 days compressive strength testing:(a) before testing and (b) after testing



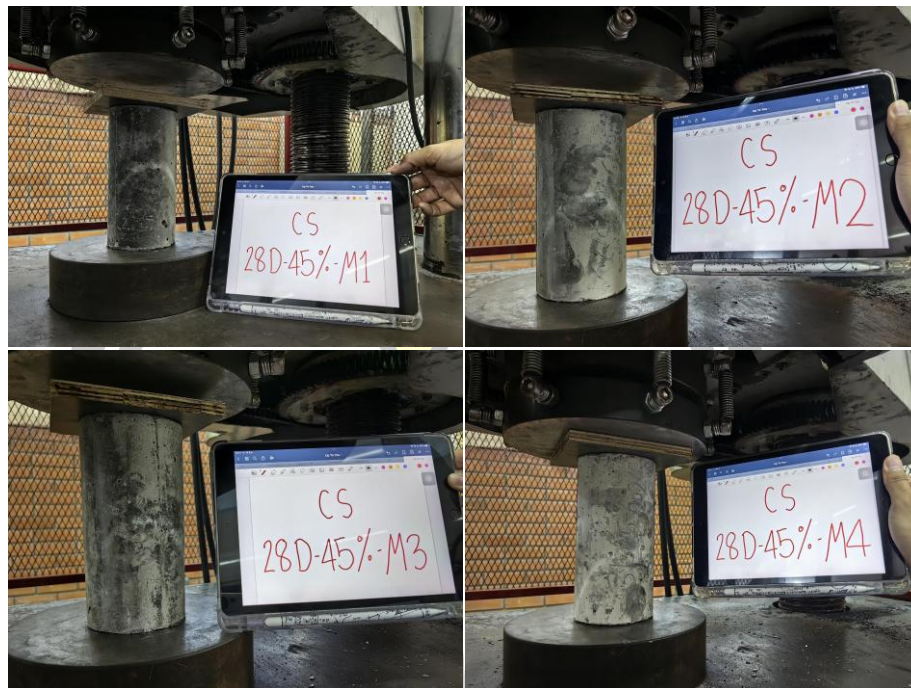


(a) Before testing



(b) After testing

Figure 38. D-M-15FA-30GS70NS samples for 28 days compressive strength testing:(a) before testing and (b) after testing



(a) Before testing

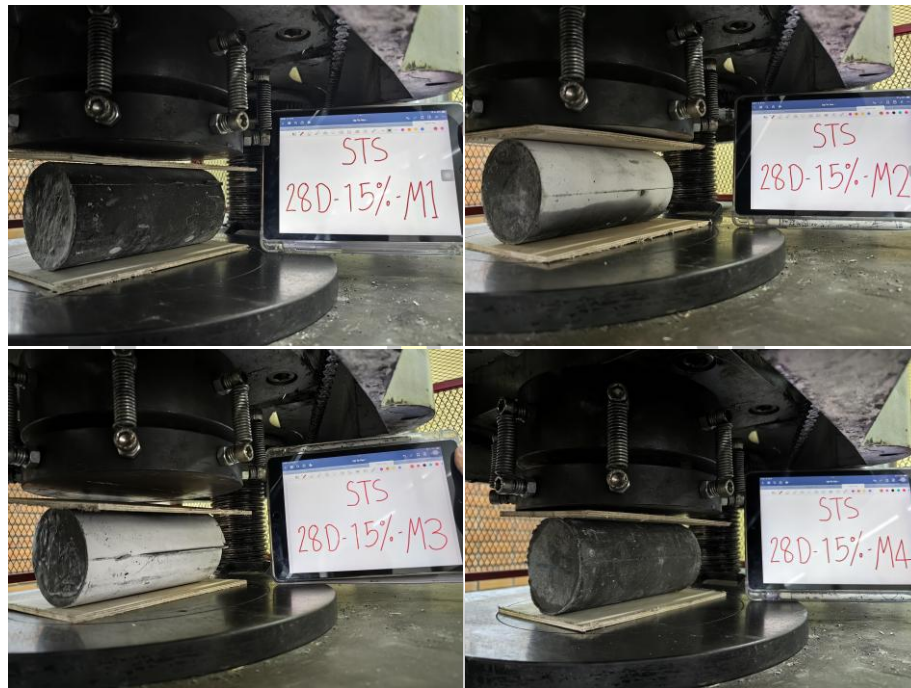


(b) After testing

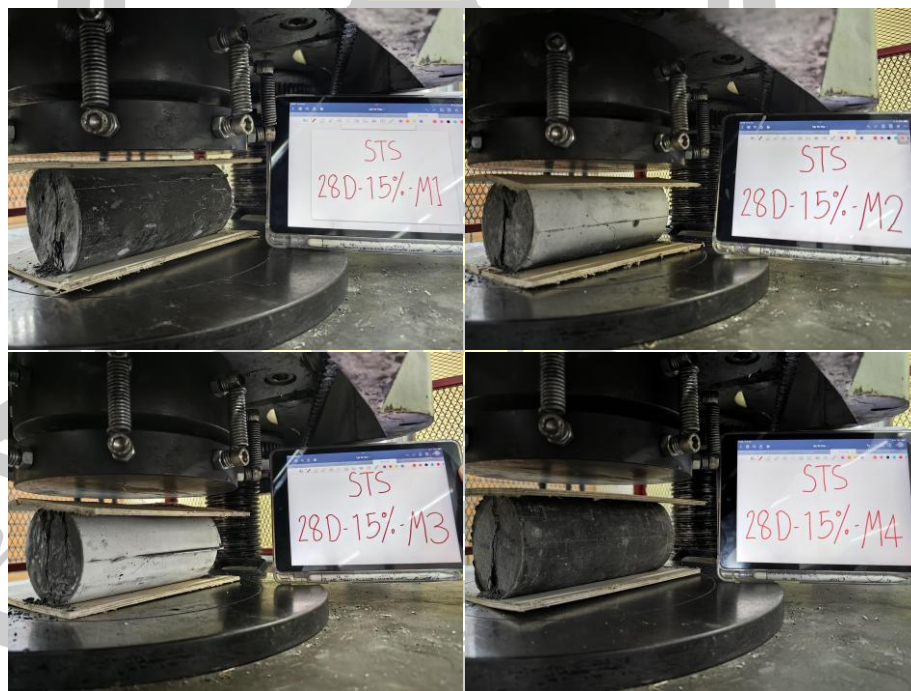
Figure 39. D-M-45FA-30GS70NS samples for 28 days compressive strength testing:(a) before testing and (b) after testing



## A2: Splitting Tensile Strength Tests



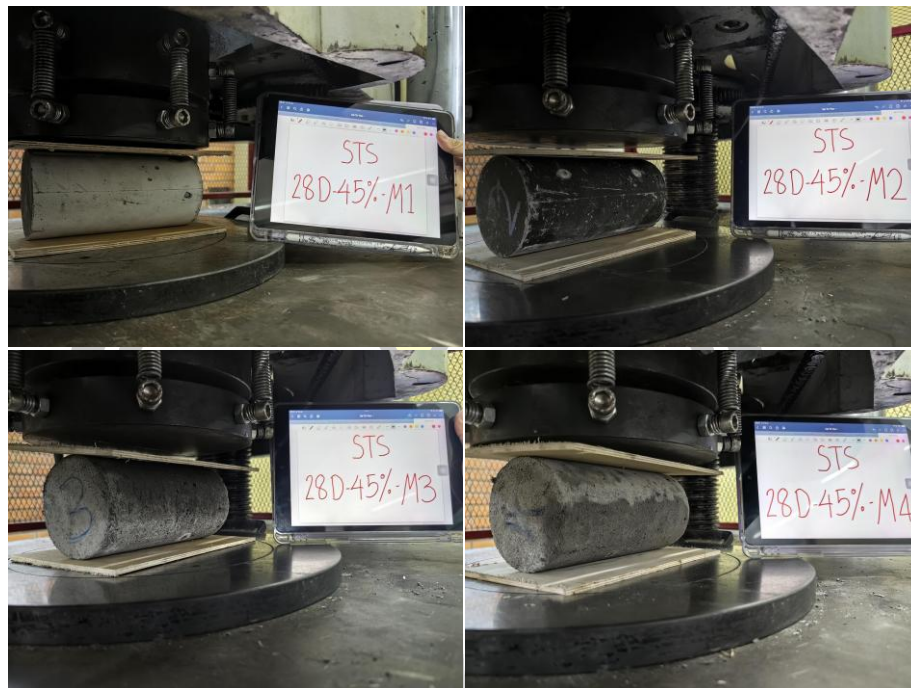
(a) Before testing



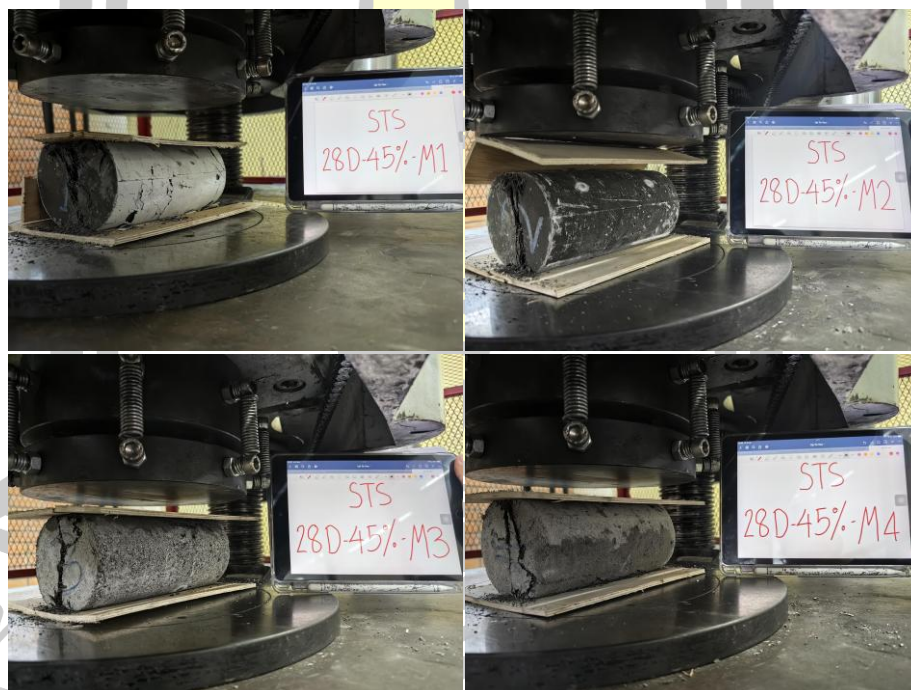
(b) After testing

Figure 40. D-M-15FA-30GS70NS samples for 28 days splitting tensile strength testing:(a) before testing and (b) after testing





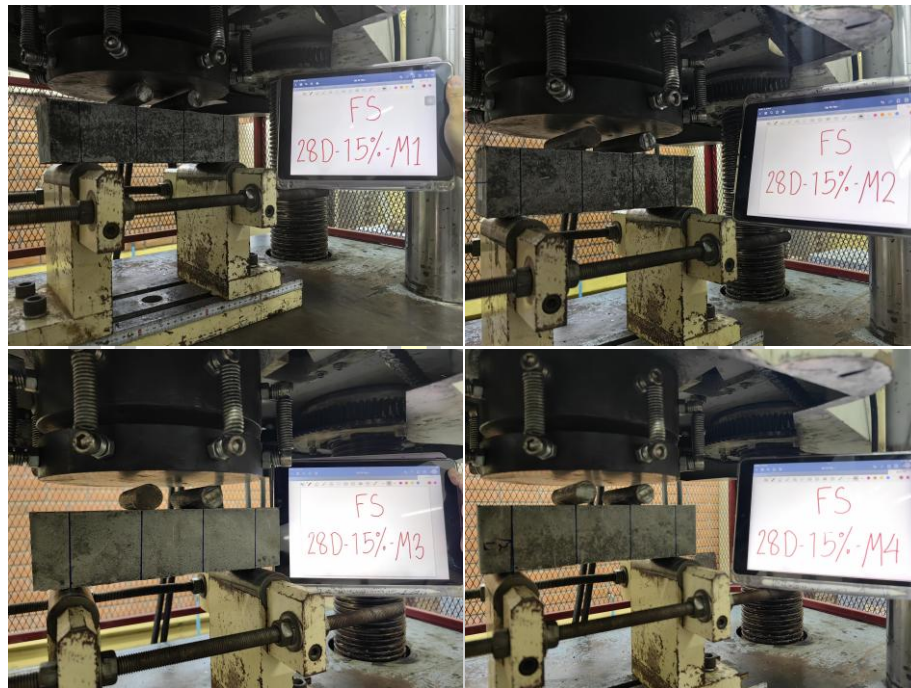
(a) Before testing



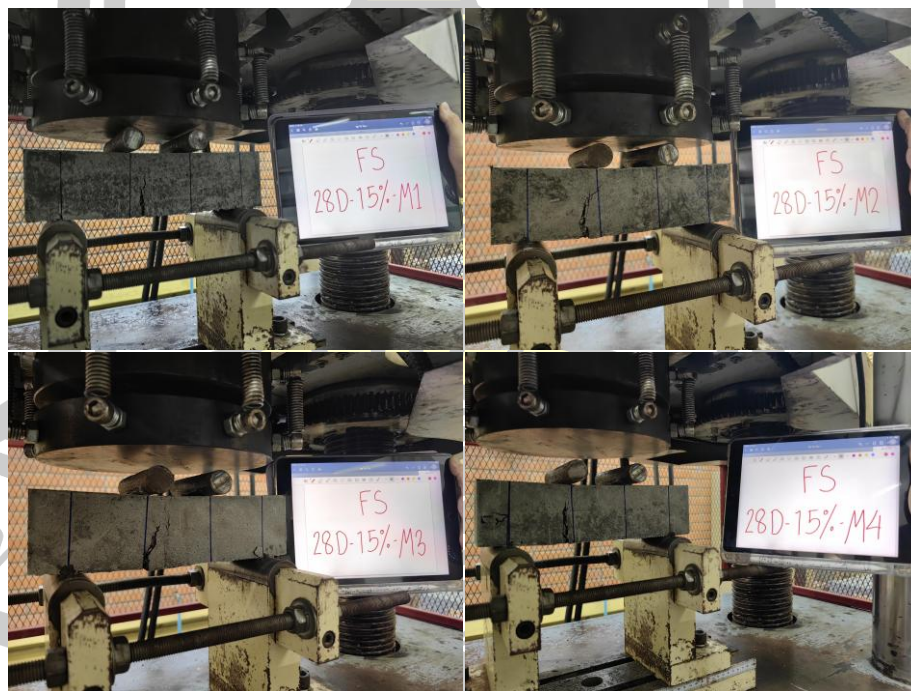
(b) After testing

Figure 41. D-M-45FA-30GS70NS samples for 28 days splitting tensile strength testing:(a) before testing and (b) after testing

### A3: Flexural Strength Tests



(a) Before testing



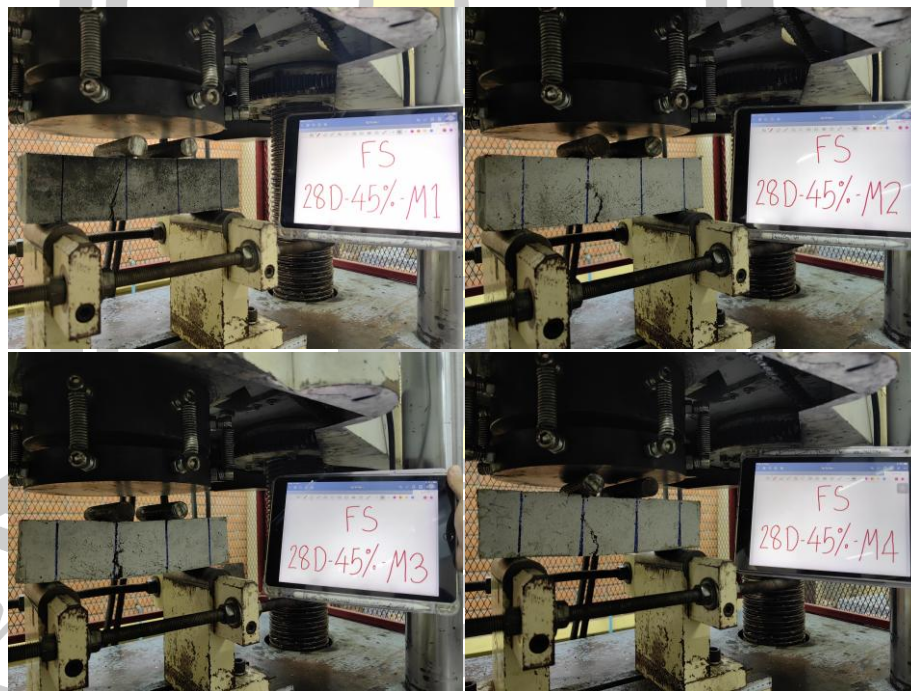
(b) After testing

Figure 42. D-M-15FA-30GS70NS samples for 28 days flexural strength testing:(a) before testing and (b) after testing





(a) Before testing



(b) After testing

Figure 43. D-M-45FA-30GS70NS samples for 28 days flexural strength testing:(a) before testing and (b) after testing

## A4: High Temperatures Tests

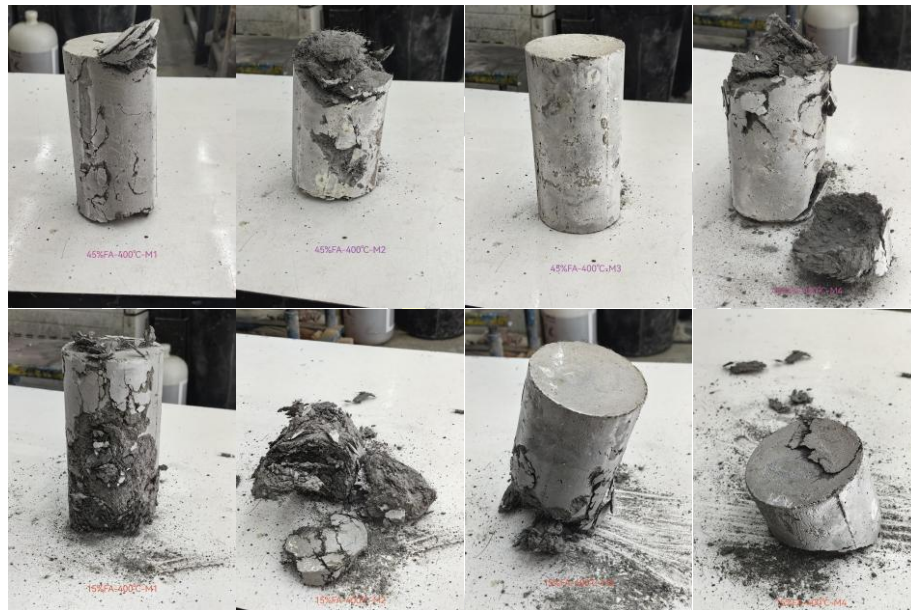


Figure 44. Post-explosion samples.

## A5: Flow Tests

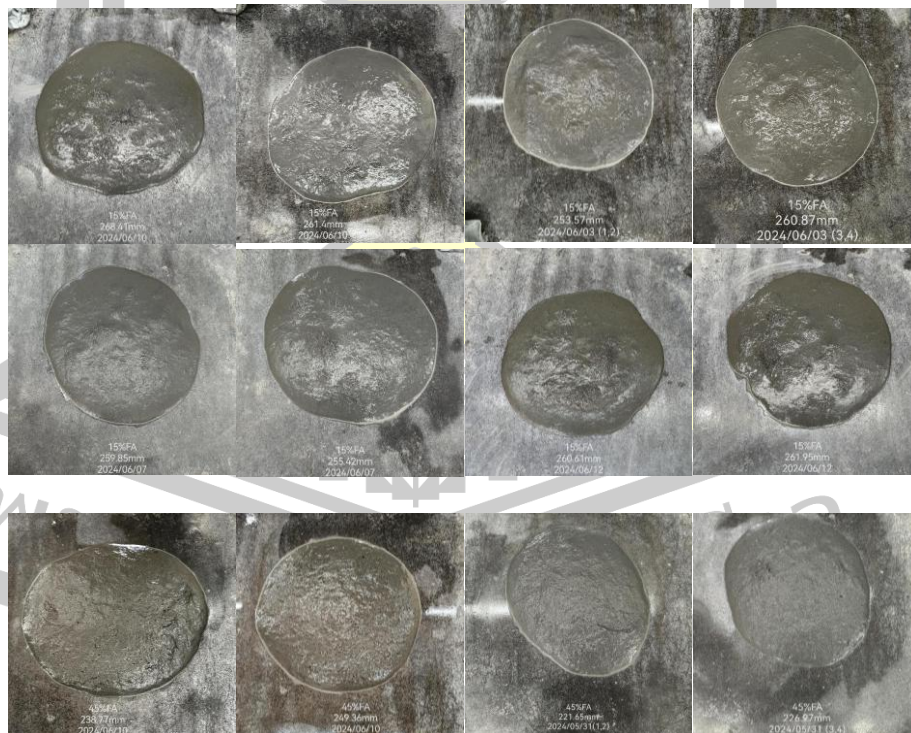






Figure 45. Flow test results.

## A6: Stress-Strain Relationship

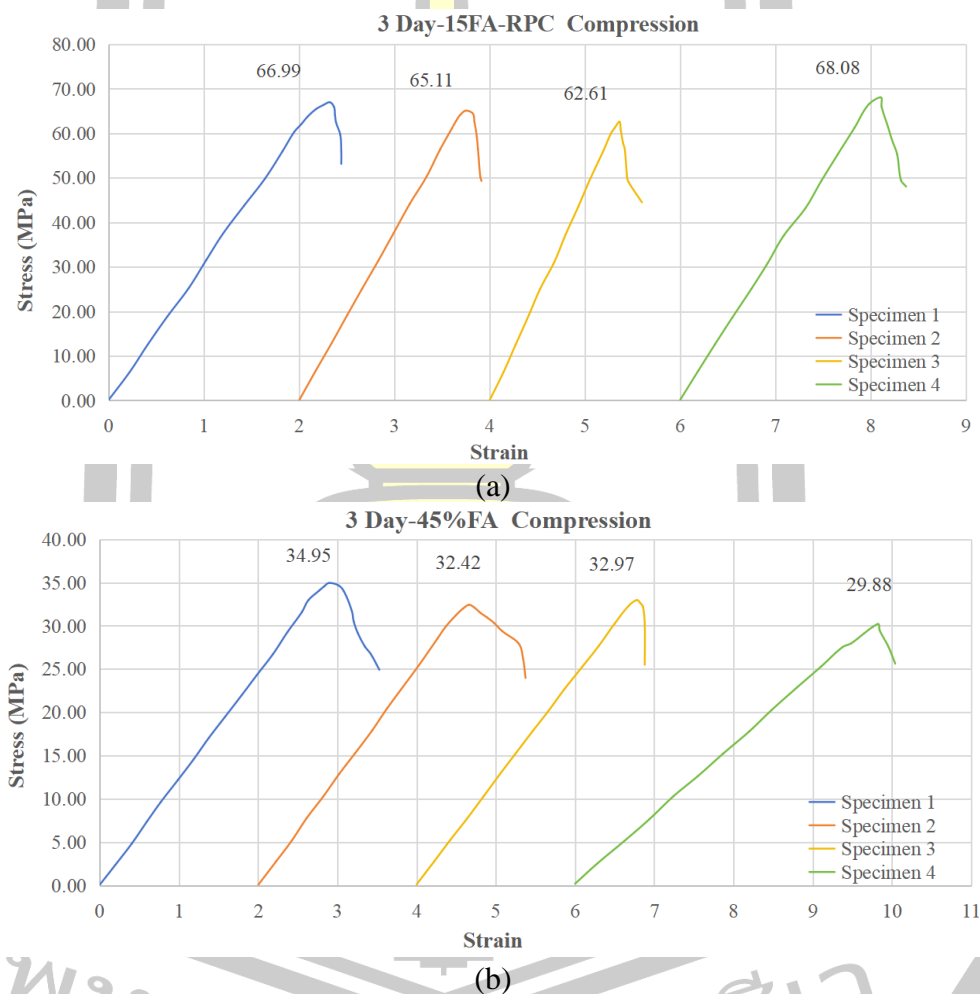


Figure 46. Stress-strain relationship of 3-day compressive strength test specimens (a) 15FA-RPC (b) 45FA-RPC.



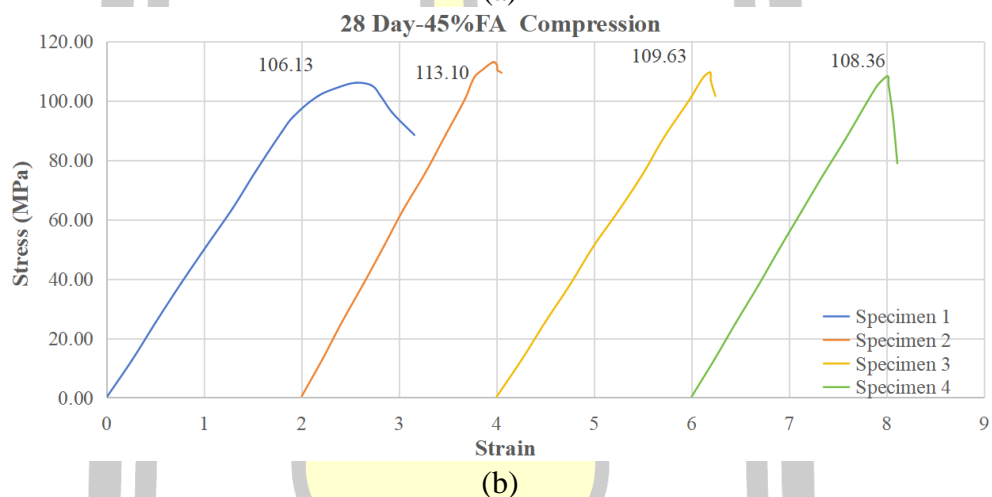
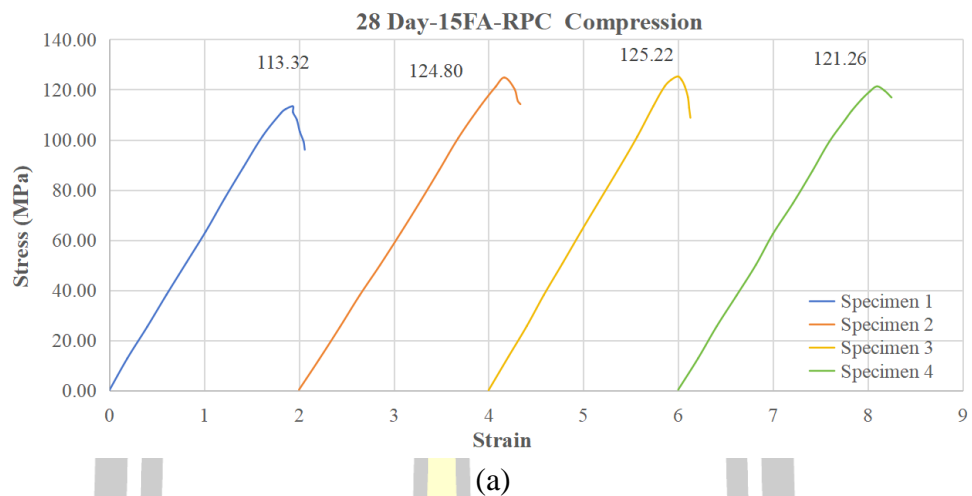
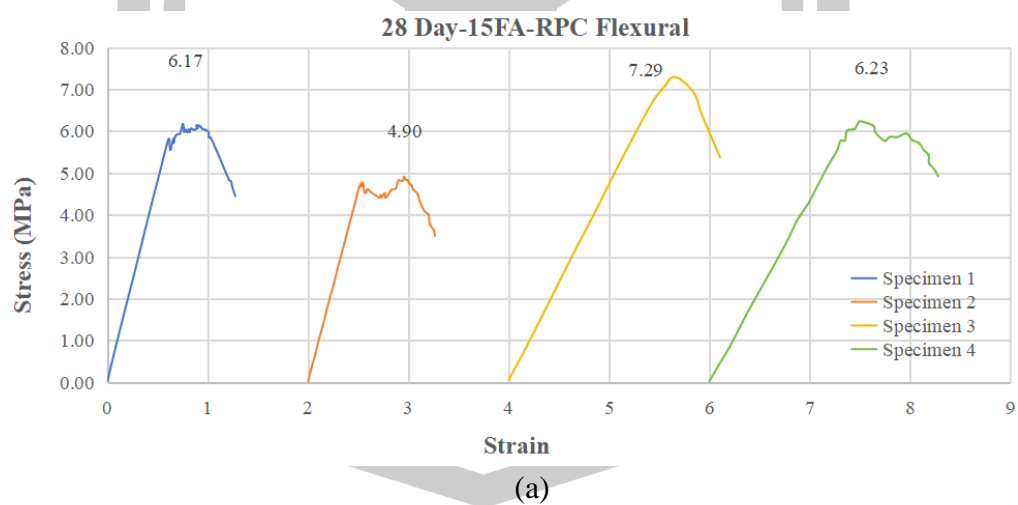
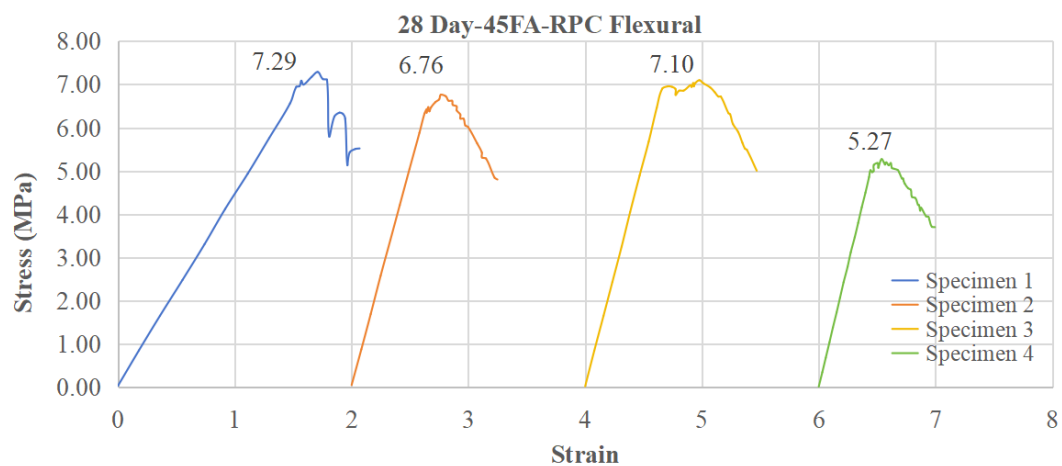
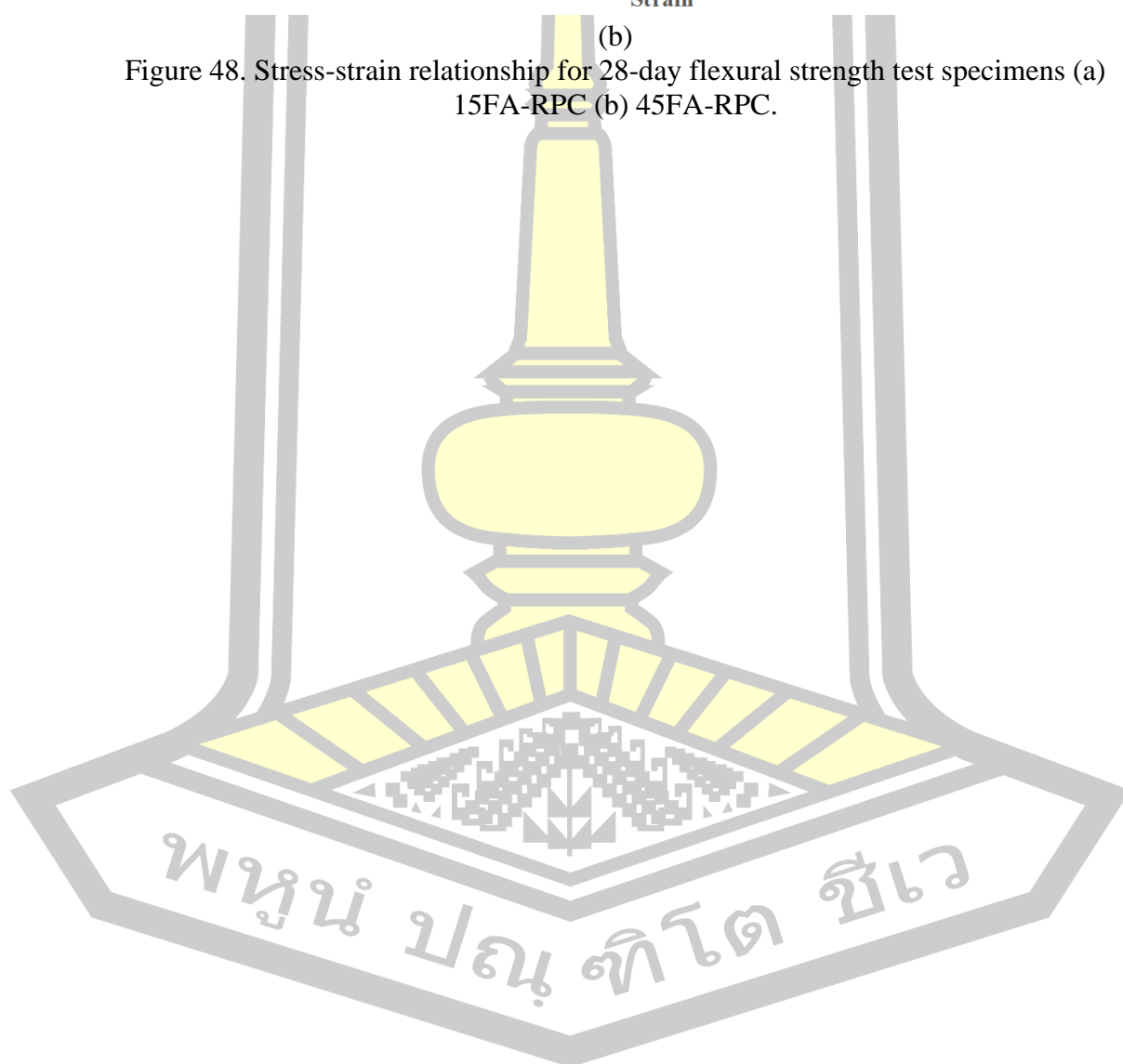


Figure 47. Stress-strain relationship of 28-day compressive strength test specimens (a) 15FA-RPC (b) 45FA-RPC.





(b)  
Figure 48. Stress-strain relationship for 28-day flexural strength test specimens (a) 15FA-RPC (b) 45FA-RPC.



## REFERENCES

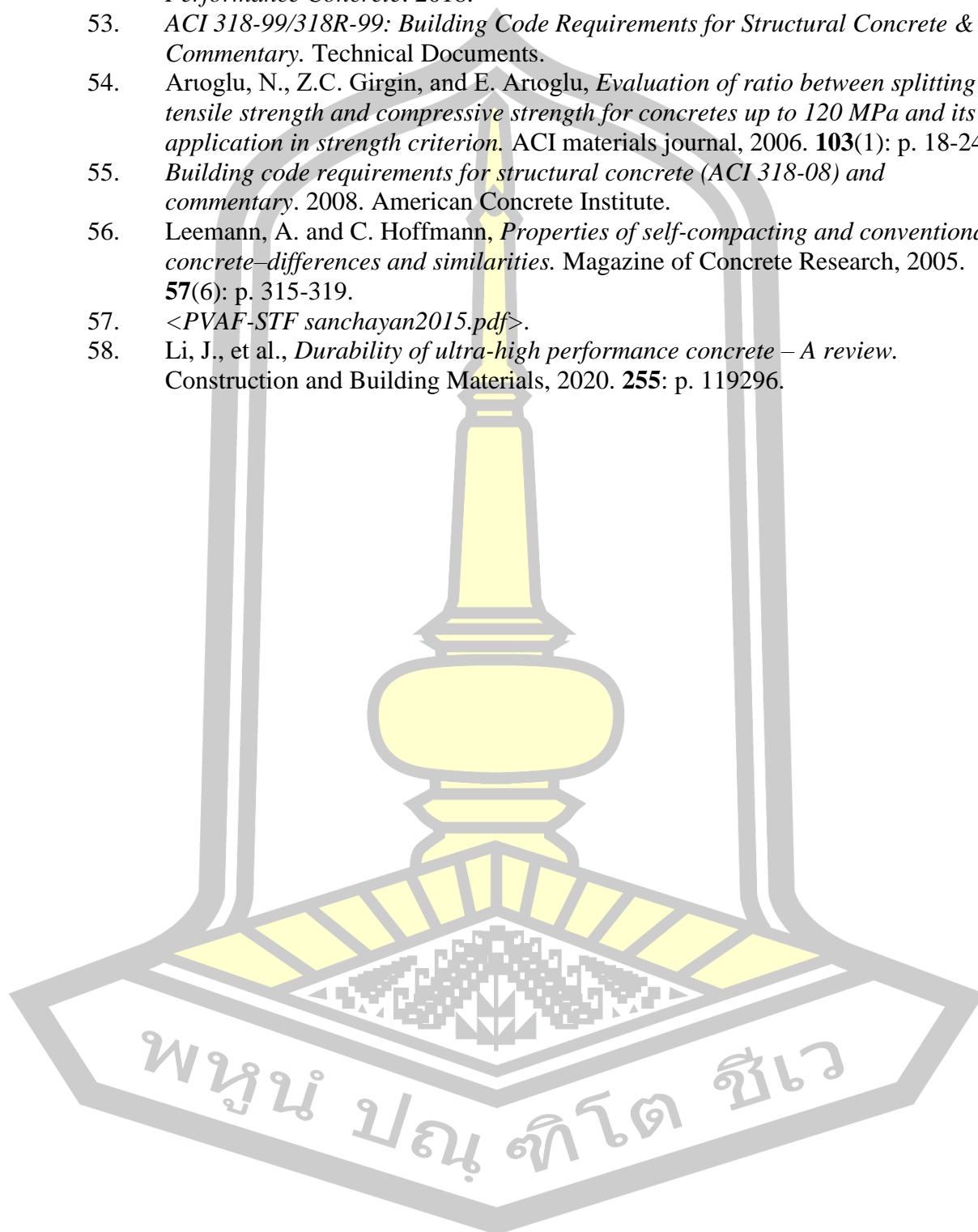
1. Wongtala, P., et al., *Experimental and numerical study on structural behavior of reactive powder concrete corbels without stirrups*. Case Studies in Construction Materials, 2023. **19**: p. e02372.
2. Richard, P. and M. Cheyrezy, *Composition of reactive powder concretes*. Cement and Concrete Research, 1995. **25**(7): p. 1501-1511.
3. Fischer, G. and V.C. Li, *Effect of fiber reinforcement on the response of structural members*. Engineering Fracture Mechanics, 2007. **74**(1): p. 258-272.
4. Yang, E.-H. and V.C. Li, *Strain-hardening fiber cement optimization and component tailoring by means of a micromechanical model*. Construction and Building Materials, 2010. **24**(2): p. 130-139.
5. Zhaopeng, Y. and L.U. Lu, *Mechanical Properties of Steel Fiber Mixed Reactive Powder Concrete*. in *Proceedings of the 2016 International Conference on Architectural Engineering and Civil Engineering*. 2016. Atlantis Press.
6. Mao, Z., et al., *Behavior evaluation of hybrid fibre-reinforced reactive powder concrete after elevated temperatures*. Construction and Building Materials, 2021. **306**: p. 124917.
7. Xia, H., W. Wang, and Z. Shi, *Mechanical properties of reactive powder concrete with ultra-short brass-coated steel fibres*. Magazine of Concrete Research, 2015. **67**(6): p. 308-316.
8. Nataraja, M.C., N. Dhang, and A.P. Gupta, *Stress-strain curves for steel-fiber reinforced concrete under compression*. Cement and Concrete Composites, 1999. **21**(5): p. 383-390.
9. Olivito, R.S. and F.A. Zuccarello, *An experimental study on the tensile strength of steel fiber reinforced concrete*. Composites Part B: Engineering, 2010. **41**(3): p. 246-255.
10. Wu, Z., et al., *Effects of steel fiber content and shape on mechanical properties of ultra high performance concrete*. Construction and Building Materials, 2016. **103**: p. 8-14.
11. Kang, S.-T., et al., *Hybrid effects of steel fiber and microfiber on the tensile behavior of ultra-high performance concrete*. Composite Structures, 2016. **145**: p. 37-42.
12. John S. Lawler, D.Z. and P.S. Surendra, *Permeability of Cracked Hybrid Fiber-Reinforced Mortar under Load*. ACI Materials Journal. **99**(4).
13. Pankaj R. Kakad, G.B.G., Rajesh R. Hetkale, Dattatray S. Kolekar Prof. Yogesh Paul, *Reactive Powder Concrete Using Fly Ash*. International Journal of Engineering Trends and Technology (IJETT), 2015. **22**: p. 4.
14. Amruta, D.A. and B.W. Anil, *Mechanical Properties of Steel Fiber Reinforced Reactive Powder Concrete Using Fly Ash*. JournalNX, 2018: p. 339-343.
15. Du, J., et al., *Modeling mixing kinetics for large-scale production of Ultra-High-Performance Concrete: effects of temperature, volume, and mixing method*. Construction and Building Materials, 2023. **397**: p. 132439.
16. Sbia, L.A., et al., *Production methods for reliable construction of ultra-high-performance concrete (UHPC) structures*. Materials and Structures, 2016. **50**(1): p. 7.
17. Mendonca, F., et al., *Feasibility study of development of ultra-high performance*

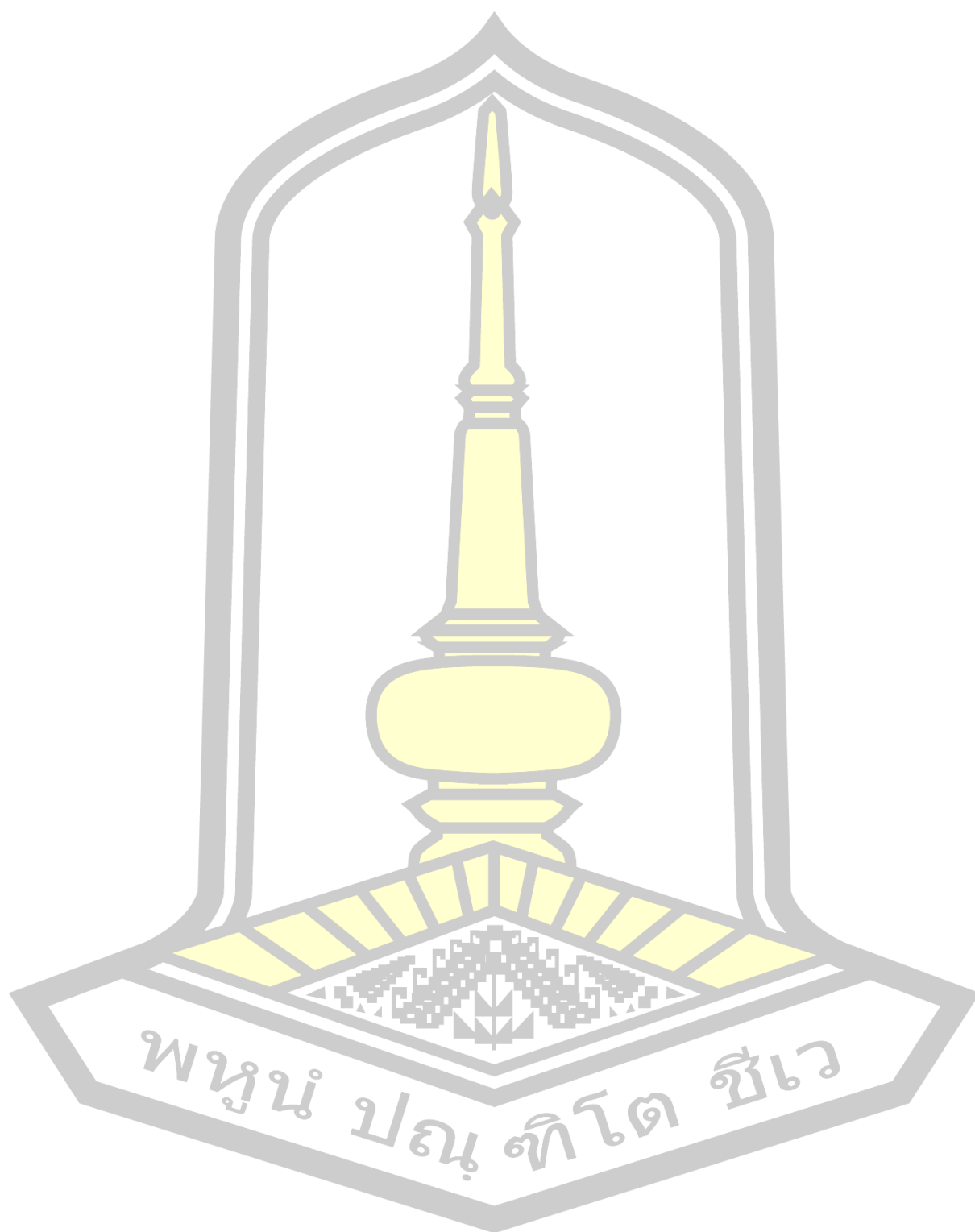
- concrete (UHPC) for highway bridge applications in Nebraska. 2020, University of Nebraska--Lincoln.
18. Amphawa, D.K.a.N., *Reactive Powder Concrete Containing Fly Ash and Coarse Aggregate*. 2023, Mahasarakham University.
  19. Huynh, T.-P., S.-H. Ngo, and V.-D. Nguyen, *A Modified Reactive Powder Concrete Made with Fly Ash and River Sand: An Assessment on Engineering Properties and Microstructure*. Periodica Polytechnica Civil Engineering, 2024. **68**(4): p. 1031–1039.
  20. J, R., *First recommendations for ultra-high-performance concretes and examples of application*. International Symposium on Ultra High Performance Concrete, 2004.
  21. Akeed, M., et al., *Ultra-high-performance fiber-reinforced concrete. Part I: Developments, principles, raw materials*. Case Studies in Construction Materials, 2022. **17**: p. e01290.
  22. Sanjuán, M.Á. and C. Andrade, *Reactive Powder Concrete: Durability and Applications*. Applied Sciences, 2021. **11**(12): p. 5629.
  23. Nili, M. and V. Afroughsabet, *Combined effect of silica fume and steel fibers on the impact resistance and mechanical properties of concrete*. International Journal of Impact Engineering, 2010. **37**(8): p. 879-886.
  24. Zheng, W.Z., et al., *Tensile Properties of Steel Fiber-Reinforced Reactive Powder Concrete after High Temperature*. Advanced Materials Research, 2012. **413**: p. 270-276.
  25. Niu, Y., J. Wei, and C. Jiao, *Crack propagation behavior of ultra-high-performance concrete (UHPC) reinforced with hybrid steel fibers under flexural loading*. Construction and Building Materials, 2021. **294**: p. 123510.
  26. Wang, Z., et al., *The Effects of Steel Fiber Types and Volume Fraction on the Physical and Mechanical Properties of Concrete*. Coatings, 2023. **13**(6): p. 978.
  27. Company, T.N.M.T., *Stainless Steel Fiber for Concrete Reinforcement with High Quality Building Material Reinforcement Resistance Steel*, in [https://s.alicdn.com/@sc04/kf/H6ed40cf58dfb4ed1a08149b6fd9399988.png\\_720x720q50.jpg](https://s.alicdn.com/@sc04/kf/H6ed40cf58dfb4ed1a08149b6fd9399988.png_720x720q50.jpg), S.S. Fiber, Editor.
  28. Tai, Y.-S., H.-H. Pan, and Y.-N. Kung, *Mechanical properties of steel fiber reinforced reactive powder concrete following exposure to high temperature reaching 800°C*. Nuclear Engineering and Design, 2011. **241**(7): p. 2416-2424.
  29. Abid, M., et al., *Effect of Fibers on High-Temperature Mechanical Behavior and Microstructure of Reactive Powder Concrete*. Materials, 2019. **12**: p. 329.
  30. Wang, C., et al., *Preparation of Ultra-High Performance Concrete with common technology and materials*. Cement and Concrete Composites, 2012. **34**(4): p. 538-544.
  31. Raza, S.S. and L.A. Qureshi, *Effect of carbon fiber on mechanical properties of reactive powder concrete exposed to elevated temperatures*. Journal of Building Engineering, 2021. **42**: p. 102503.
  32. Sbia, L., et al., *Enhancement of Ultra High Performance Concrete Material Properties with Carbon Nanofiber*. Advances in Civil Engineering, 2014. **2014**: p. 10.
  33. Abdelrahim, M., et al., *Effect of Steel Fibers and Temperature on the*

- Mechanical Properties of Reactive Powder Concrete*. Civil and Environmental Engineering, 2021. **17**: p. 000010247820210028.
34. Yu, R., P. Spiesz, and H.J.H. Brouwers, *Development of an eco-friendly Ultra-High Performance Concrete (UHPC) with efficient cement and mineral admixtures uses*. Cement and Concrete Composites, 2015. **55**: p. 383-394.
  35. Yunsheng, Z., et al., *Preparation of C200 green reactive powder concrete and its static–dynamic behaviors*. Cement and Concrete Composites, 2008. **30**(9): p. 831-838.
  36. Ju, Y., et al., *Influence of steel fiber and polyvinyl alcohol fiber on properties of high performance concrete*. Structural Concrete, 2022. **23**(3): p. 1687-1703.
  37. Al-tikrite, A. and M. Hadi, *Mechanical properties of reactive powder concrete containing industrial and waste steel fibres at different ratios under compression*. Construction and Building Materials, 2017. **154**: p. 1024-1034.
  38. Ju, Y., et al., *Mesomechanism of steel fiber reinforcement and toughening of reactive powder concrete*. Science in China Series E: Technological Sciences, 2007. **50**(6): p. 815-832.
  39. Abid, M., et al., *High temperature and residual properties of reactive powder concrete – A review*. Construction and Building Materials, 2017. **147**: p. 339-351.
  40. Ju, Y., et al., *An experimental investigation of the thermal spalling of polypropylene-fibered reactive powder concrete exposed to elevated temperatures*. Science Bulletin, 2015. **60**(23): p. 2022-2040.
  41. Sanchayan, S. and S.J. Foster, *High temperature behaviour of hybrid steel–PVA fibre reinforced reactive powder concrete*. Materials and Structures, 2016. **49**(3): p. 769-782.
  42. Sai Sree, K.S. and S. Koniki, *Mechanical Properties of PVA & Steel Hybrid Fiber Reinforced Concrete*. E3S Web Conf., 2021. **309**: p. 01174.
  43. Sun, Q., et al., *Influence of different grinding degrees of fly ash on properties and reaction degrees of geopolymers*. PLOS ONE, 2023. **18**(3): p. e0282927.
  44. Anjeza Alaj, V.K., Tatsuya Numao, *Effect of Class F Fly Ash on Strength Properties of Concrete*. 2023. **9**.
  45. Sevim, Ö. and İ. Demir, *Physical and permeability properties of cementitious mortars having fly ash with optimized particle size distribution*. Cement and Concrete Composites, 2019. **96**: p. 266-273.
  46. Stefanović, G., et al., *Hydration study of mechanically activated mixtures of Portland cement and fly ash*. Journal of the Serbian Chemical Society, 2007. **72**.
  47. Committee, A.C.I., *Use of Fly Ash in Concrete*. ACI Materials Journal. **84**(5).
  48. Babalu, R., et al., *Compressive strength, flexural strength, and durability of high-volume fly ash concrete*. Innovative Infrastructure Solutions, 2023. **8**(5): p. 154.
  49. Muhsin, Z.F. and N.M. Fawzi, *Effect of Fly Ash on Some Properties of Reactive Powder Concrete*. Journal of Engineering, 2021. **27**(11): p. 32-46.
  50. Chong, W., et al., *Behavior and Mechanism of Pozzolanic Reaction Heat of Fly Ash and Ground Granulated Blastfurnace Slag at Early Age*. Journal of the Chinese Ceramic Society, 2012. **40**(7): p. 1050-1058(9).
  51. Zhang, J., et al., *Reaction mechanism of sulfate attack on alkali-activated slag/fly ash cements*. Construction and Building Materials, 2022. **318**: p. 126052.



52. El-Tawil, S., et al., *Commercial Production of Non-Proprietary Ultra High Performance Concrete*. 2018.
53. *ACI 318-99/318R-99: Building Code Requirements for Structural Concrete & Commentary*. Technical Documents.
54. Arioglu, N., Z.C. Girgin, and E. Arioglu, *Evaluation of ratio between splitting tensile strength and compressive strength for concretes up to 120 MPa and its application in strength criterion*. *ACI materials journal*, 2006. **103**(1): p. 18-24.
55. *Building code requirements for structural concrete (ACI 318-08) and commentary*. 2008. American Concrete Institute.
56. Leemann, A. and C. Hoffmann, *Properties of self-compacting and conventional concrete—differences and similarities*. *Magazine of Concrete Research*, 2005. **57**(6): p. 315-319.
57. <PVAF-STF sanchayan2015.pdf>.
58. Li, J., et al., *Durability of ultra-high performance concrete – A review*. *Construction and Building Materials*, 2020. **255**: p. 119296.





## BIOGRAPHY

NAME	Jinhao Wei
DATE OF BIRTH	1994/07/21
PLACE OF BIRTH	HENAN
ADDRESS	Building 4, Didu International City Community, Luolong District, Luoyang City, Henan Province, China
EDUCATION	Bachelor of Engineering; Xi'an University of Architecture and Technology Master of Engineering; Mahasarakham University

